BACHELOR'S THESIS

Degree in Mathematics

Title: Interference of defective particles in the replication of RNA viruses with satellites

Author: Ariadna Albó Delgado

Advisors: Jose Tomás Lázaro Ochoa, Josep Sardanyés Cayuela and Santiago Elena

Department: Mathematics Department

Academic year: 2017-2018

UNIVERSITAT POLITÈCNICA DE CATALUNYA
BARCELONATECH
Facultat de Matemàtiques i Estadística

Interference of defective particles in the replication of RNA viruses with satellites

Ariadna Albó, S.F. Elena, J.T. Lázaro and J. Sardanyés

September 4, 2018

Thanks to Tomás Lázaro and Josep Sardanyés.
Without your help it would not have been possible the realization of this project.

Abstract

In this project we have investigated a dynamical system describing the dynamics of a standard virus together with its defective interfering particles (DIPs) and a virus satellite. Our model is inspired in the hepatitis B Virus (HBV) - hepatitis Delta Virus (HDV) system, which is currently a major health problem. The HDV is a virus satellite that co-infects with HBV. Double infections with HBV-HDV usually involve a greater impact on patients health. Mathematical models on HBV-HDV systems are scarce in the literature, especially under the impact of the DIPs. DIPs are incomplete virus that typically interfere with the replication of the standard virus (HBV). They have been suggested as possible therapeutic agents decreasing standard viruses fitness. Our model, as far as we know, is the first attempt to describe the dynamics of this 3-virus system, with the standard virus being accompanied by the satellite, together with the DIPs synthesised by the standard virus. We have built a mathematical model based on ordinary nonlinear differential equations, modelling the population dynamics of the three virus types under the processes of competition and interference of DIPs. We have computed the equilibrium points, providing the conditions for the extinction and coexistence of the populations. We have identified transcritical bifurcations involving the transition from a satellite-free scenario i.e., coexistence standard virus-DIPS, to the extinction of the three viral types. Our analytic and numerical results focus on the stability of the system giving place to different scenarios which are relevant from a biomedical point of view.

Keywords: virus, defective interfering particles, virus satellite, bifurcation, stability

Contents

1 Introduction

Viruses are among the smallest replicators also being important pathogens for bacteria, fungi, plants and animals. Viruses are obligate parasites lacking translation machinery to complete their infection cycles. Hence, they need to infect and take profit of the host cellular machinery to replicate their genomes and produce the structural proteins that will be used for encapsulating their genomes. These pathogens are extremely diverse and they present many different shapes, genetic architectures, and varied life cycles. Viruses are typically composed by a protein-made capsid which contains the viral genome (DNA and/or RNA). The genome can be a single or a double RNA strand, a DNA molecule, or different RNA genomes that can be encapsulated together in the same viral particle (segmented viruses e.g., influenza) or in different viral particles (multipartite viruses e.g., alphalpha mosaic virus). Interestingly, some types of viruses can interact with so-called virus satellites [1], which are subviral agents composed of a nucleic acid that depends on the co-infection of a host cell by the standard virus (regular virus able to complete the whole infection cycle by its own) for its replication.

Satellite viruses, which are most commonly associated with plants [1], can also infect bacteria, arthropods, and mammals. The first satellite virus was discovered in 1962, and it is believed that these viruses may have emerged from either the genome of the host or its co-infecting agents, or any vectors leading to transmission [1]. As mentioned, these viruses have the components to make their own protein capsid but depend on the so-called standard virus. As a difference from the standard virus, which has the capability to use host proteins for replication, satellite viruses can not complete their infection cycle alone. In other words, satellite virus can not replicate their genomes without co-infection with a standard virus. Typically, virus satellites have been suggested to establish symbiotic relations with the standard host virus, thus getting a benefit. However, other side-effect processes such as competition may arise during co-infection. Moreover, some satellite viruses can also act as parasites of the standard virus, thus taking a profit of the presence of the standard virus but not providing an advantage to it.

Hepatitis B virus (HBV) infection is a serious global health problem, with 2 billion people infected worldwide, and 350 million suffering from chronic HBV infection. Being the 10th leading cause of death worldwide, HBV infections result in 500.000 to 1.2 million deaths per year caused by chronic hepatitis, cirrhosis, and hepatocellular carcinoma. HBV is transmitted through contact with infected blood or semen. In areas of high endemicity, the virus is transmitted mostly perinatally from infected mothers to neonates, and in low endemic areas sexual transmission is predominant. Risk of infection is higher in people who have different sexual partners, men who have sex with other men, unsafe injections, blood transfusions, or dialysis. Household or intimate non-sexual contact and living in crowded conditions are also possible risks.

Acute HBV infection is age dependent: roughly 95% of neonates, 20-30% of children (1-5 years) and less than 5% of adults develop chronic infection. Prevention of perinatal transmission of HBV is crucial,

because the risk of progression from acute to chronic HBV infection is 90% when infection occurs in infants. An effective vaccine against this infection is available since 1981 and since the introduction of it and other preventive measures, the worldwide prevalence of hepatitis B infection has fallen. Most vaccines are made from recombinant DNA that expresses HBsAg only.

Hepatitis B virus belongs to the *Hepadnaviridae* family. It is a partly doublestranded DNA virus. The transcriptional template of HBV is the cccDNA, which resides inside the hepatocyte nucleus as a minichromosome. The replication of HBV involves the packaging and reverse transcription of an RNA intermediate. The existence of spliced HBV RNAs has been demonstrated but their significance is not clear. It has been found that splicing of HBV RNA, followed by reverse transcription and packaging, leads to secretion in serum of defective HBV particles (DIPs).

Satellite viruses also have an important impact on human health. For instance, the Hepatitis D (or Delta) Virus (HDV). Hepatitis viruses infect hepatic cells in the liver and are a major health problem. HDV was discovered in 1977 by Mario Rizzetto [2], who found a new nuclear agent in the liver cells of patients infected with Hepatitis B Virus (HBV). This new agent was thought to be a new protein encoded by HBV, and it was labeled as the delta antigen. Further research on chimpanzees, however, indicated that this antigen was derived from a new virus, named the HDV. As a difference from the other hepatitis viruses, such as Hepatitis A or C, HDV needs to co-infect with HBV or needs to infect people with chronic HBV infection (process called superinfection). Hepatitis C and D viruses are RNA viruses, while HBV is a DNA one. Hepatitis Delta virus consists of a single-stranded, negative-sense, circular RNA genome, with an envelope made up of HBAg (Hepatitis B Antigen). The viral particles (also called virions) are 35-43 nm long and are roughly spherical. The capsid proteins are the only proteins encoded by HDV genome. HDV replication occurs in the nucleus of primary hepatocytes (liver cells). Importantly, new HDV virions can only be assembled under the presence of HBV.

Hepatitis Delta virus infections are found worldwide, but the prevalence differs in different geographical areas, being high in Africa, the Middle East, and Southern Italy. Worldwide, over 10 million people are infected with HDV. When chronic HBV carriers are infected with HDV, an 80 % of the cases suffer acute hepatitis and chronic Hepatitis infection. Under this situation, the so-called fulminant viral hepatitis is about ten-fold more common in HDV infections than in the other types. Fulminant hepatitis is characterized by hepatic encephalopathy manifested in changes of personality, disturbances in sleep, confusion, abnormal behaviour, and coma. The mortality rate of fulminant hepatitis is about 80% [2]. Moreover, chronic HDV infection typically progresses to liver cirrhosis in about 60-70% of patients. Hepatocellular carcinoma (liver cancer) occurs in chronically infected HDV patients with the same frequency as in patients only infected with HBV. Overall, the mortality rates for HDV infection lines between 2% and 20%, values ten times greater than the mortality rates for only-HBV infected people [2].

It is known that viruses can produce the so-called defective interfering particles (hereafter DIPs) during their replication. DIPs were first reported by Von Magnus [3], who studied their development in Influenza A virus populations passaged in embryonated chicken eggs. Based on these serial passage experiments the existence of incomplete virus variants which increase rapidly in frequency and cause drops in overall virus titers was proposed. The existence of virus variants with large genomic deletions has since been confirmed in many virus families [4], including the Alphabaculoviruses [5]-[8]. DIPs viruses are generated almost instantly and accumulate rapidly when baculoviruses are introduced into cultured insect cells [7]-[8], leading to problems with sustained expression of heterologous proteins [7] in this widely used expression system [9]. DIPs viruses are thought to replicate much faster than viruses with a full-length genome, due to their smaller genome sizes. Moreover, DIPs can evolve other strategies to better compete with standard viruses, such as the accumulation of origins of DNA replication within a single genome [10]-[12], a phenomenon that can be cell-line dependent [12]. On the other hand, DIPs cannot autonomously replicate because they lack essential genes. They must therefore co-infect a cell with a standard virus in order to replicate, becoming obligate parasites of standard viruses, as they must co-opt gene products and cannot replicate on their own. When the frequency of the DIPs is high, overall virus production is low because essential gene products, which must come from a helper virus, are no longer available (i.e., interference). DIPs can have implications for virus amplification in cultured cells, protein expression using viral vectors, and vaccination [13]. DIPs are produced by almost all RNA viruses, which have very large mutation rates and thus are prone to synthesize defective genomes during replication. Examples of DIPs have been described in RNA viruses such as vesicular stomatitis virus (VSV) [13]-[14] and baculoviruses [6]-[12].

Interestingly, DIPs can also be produced by DNA viruses such as HBV. Defective forms of HBV, named spliced HBV, have been characterized and investigated *in vivo* [15]-[16]. Theoretical investigations of the dynamical impact of DIPs in the replication of standard viruses have been carried out by several authors [17]-[20]. Typically, these mathematical models have been studied with mean-field approximations considering either discrete- [17]-[18] or continuous-time [19]-[20] dynamical systems. To the extend of our knowledge, the interference of DIPs in satellite viruses co-infecting with standard viruses have not been explored to date. This is the topic of this research project. We are interested in characterizing the dynamics and the potential bifurcations in a system composed by a standard virus (HBV), its satellite (HDV), and the DIPs generated by the standard virus. Hence, these will be the state variables of the dynamical system investigated in this project.

This can have therapeutic implications due to the competence between the DIP and the HBV, and also the satellites can interfere with the virus.

2 Mathematical model

We develop a model based on ordinary differential equations to investigate the dynamics of viruses with satellites affected by the so-called defective interfering particles (DIPs). We are particularly interested in a specific systems given by hepatitis B virus (HBV). This virus is known to carry RNA satellites.
Let us denote by $x = (v, s, D)$ the following state variables denoting the population numbers of:

v : standard virus
s : virus satellites
D : Defective Interfering Particles (DIPs).

Consider also the following list of parameters involved in the model:

α : replication rate of standard virus
η : interference strength of satellites on the replication of standard viruses
η_D : interference strength of DIPs on the replication of standard viruses
β : replication rate of virus satellites
ε : decay rate of the viral particles
μ : production rate of DIPs
γ : DIPs replication rate.

An schematic representation of such model is given in Fig. 1. The corresponding system of differential equations is given by

$$\dot{v} = \alpha(1-\mu)v\,\Omega(x) - \varepsilon v \tag{1}$$
$$\dot{s} = \beta v s\,\theta(x) - \varepsilon s \tag{2}$$
$$\dot{D} = (\alpha\mu v + \gamma v D)\,\theta(x) - \varepsilon D, \tag{3}$$

where

$$\Omega(x) = 1 - v - \eta s - \eta_D D,$$
$$\theta(x) = 1 - v - s - D,$$

with the hypotheses

$$0 < \mu \ll 1, \qquad \eta_D \geq \eta > 1, \qquad \gamma \geq \alpha$$

We will also assume that $\gamma > \beta - 1$.

Biologically, $0 < \mu \ll 1$ because DIPs are produced by DNA viruses and its replication does not have many errors, $\eta_D \geq \eta > 1$ due to interference of DIPs is greater than satellites', and $\gamma \geq \alpha$ since the genome of DIPs is shorter than the viruses' and then the formation cycle of the first ones is faster.

On the other hand, $\Omega(x)$ and $\theta(x)$ are logistic functions that introduce the competence between viral populations.

Remark 2.1 *Remember that a logistic differential equation takes the form*

$$\dot{x} = kx\left(1 - \frac{x}{m}\right),$$

where k denotes the growth rate and m the carrying capacity.

In the following lines we describe some of the parameters in equations (1)-(3) to better understand our model. As virus v creates viruses and DIPs, in equation (1), the factor $(1-\mu)$ determines the fraction of virus that creates virus and, multiplying it by α, it determines the replication rate of that part of virus. Since the satellites and the DIPS need the standard virus to replicate, βvs and γvD in equations (2) and (3) denote the relation between the two involved variables. Factor $\alpha\mu v$ determines the relation between the replication of standard virus and the production of DIPS. Finally, $-\varepsilon v$, $-\varepsilon s$ and $-\varepsilon D$ denote the decay of virus, satellite and DIP, respectively.

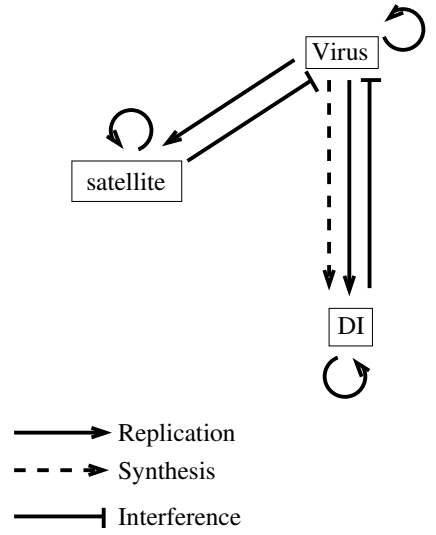

Figure 1: Hepatitis B and its Hepatitits-δ satellite model. While the virus can replicate itself, the satellite need the standard virus to do it. Moreover, HBV synthesises DIP, which also needs the virus to replicate.

This study has been divided in different parts. Broadly, we have a first section where we study the dynamically relevant domain of our system. The following sections determine the different kind of equilibrium points in our model and also study their stability and bifurcation values where the stability changes. Finally, the last section is the study of the dynamics onto the border of our interesting domain.

3 Confinement and dynamically relevant domain

Let us consider our main system. Remind that

$$\begin{aligned}\dot{v} &= \alpha(1-\mu)v\,\Omega(x) - \varepsilon v,\\ \dot{s} &= \beta v s\,\theta(x) - \varepsilon s,\\ \dot{D} &= (\alpha\mu + \gamma D)\,v\theta(x) - \varepsilon D,\end{aligned}$$

where $\Omega(x)$ and $\theta(x)$ are already defined:

$$\begin{aligned}\Omega(x) &= 1 - v - \eta s - \eta_D D,\\ \theta(x) &= 1 - v - s - D,\end{aligned}$$

In vector form, it is equivalent to $\dot{x} = F(x)$, where $x = (v, s, D)$ and provided we define

$$F(x) = \begin{pmatrix} \alpha(1-\mu)v\,\Omega(x) - \varepsilon v \\ \beta v s\,\theta(x) - \varepsilon s \\ (\alpha\mu + \gamma D)\,v\theta(x) - \varepsilon D \end{pmatrix}.$$

The variables v, s, and D have biological meaning only if they are non-negative. Therefore it is reasonable to consider them on $\mathcal{Q} := \{(v, s, D) \mid v \geq 0, s \geq 0, D \geq 0\}$. Since $\eta_D \geq \eta > 1$ it is clear that $\Omega(x) \leq \theta(x)$ on $\mathcal{Q}$. Furthermore, equality is reached if and only if $x = (v, s, D) = (1, 0, 0)$. This means that the plane $\{\Omega(x) = 0\}$ divides the tetrahedron $\mathcal{T}$ defined by the coordinate planes and the plane $\{\theta(x) = 0\}$ in two regions (see Fig. 2):

(I) $\{\Omega(x) > 0\} \cap \{\theta(x) > 0\}$

(II) $\{\Omega(x) < 0\} \cap \{\theta(x) > 0\}$.

The exterior of the tetrahedron included in $\mathcal{Q}$ is given by $\{\Omega(x) < 0\} \cap \{\theta(x) < 0\}$. Notice that

$$\begin{aligned}\Omega(x) = 0 &\quad\Leftrightarrow\quad v + \eta s + \eta_D D = 1,\\ \theta(x) = 0 &\quad\Leftrightarrow\quad v + s + D = 1.\end{aligned}$$

Lemma 3.1 *The tetrahedron $\mathcal{T}$ is invariant under the flow of F. The vector field F points (a) inwards on $\{\theta(x) = 0\}$; (b) towards the interior of $\mathcal{T}$ on $\{D = 0\}$ and (c) makes invariant the planes $\{v = 0\}$ and $\{s = 0\}$. In particular, this implies that $\mathcal{T}$ contains the dynamics for large positive times.*

Proof. Let define $\Pi := \{\theta(x) = 0\} \setminus \{(1, 0, 0)\}$. Observe that, in other words, $\Pi = \{v + s + D = 1\}$ except the point $(1, 0, 0)$. The vector field F onto Π becomes

$$F|_\Pi = \begin{pmatrix} \alpha(1-\mu)v\Omega(x) - \varepsilon v \\ -\varepsilon s \\ -\varepsilon D \end{pmatrix}.$$

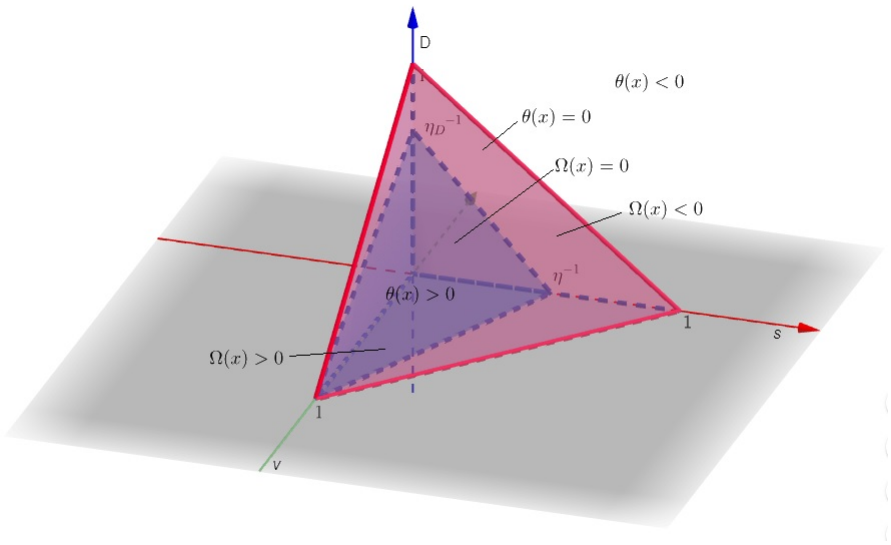

Figure 2: Dynamical essential regions in the tetrahedron $\mathcal{T}$, i.e. the phase space of our system.

Since $\Omega(x) < \theta(x)$ on Π, it follows that $\alpha(1-\mu)v\Omega(x) - \varepsilon v < 0$, and so F points inwards.
On the other hand,

$$F|_{\{v=0\}} = \begin{pmatrix} 0 \\ -\varepsilon s \\ -\varepsilon D \end{pmatrix} \in \{v = 0\} \Longrightarrow \{v = 0\} \text{ is } F\text{-invariant.}$$

Similarly,

$$F|_{\{s=0\}} = \begin{pmatrix} \alpha(1-\mu)v\Omega(v,0,D) - \varepsilon v \\ 0 \\ (\alpha\mu + \gamma D)v\theta(v,0,D) - \varepsilon D \end{pmatrix} \in \{s = 0\} \Longrightarrow \{s = 0\} \text{ is also } F\text{-invariant.}$$

Moreover,

$$F|_{\{D=0\}} = \begin{pmatrix} \alpha(1-\mu)v\Omega(v,s,0) - \varepsilon v \\ \beta vs\theta(v,s,0) - \varepsilon s \\ \alpha\mu v\theta(v,s,0) \end{pmatrix}.$$

Its third component is positive except if $v = 0$ or $v + s = 1$ so it points inwards $\mathcal{T}$. In particular, on $\{D = 0, v + s = 1\}$, the vector field F becomes

$$\begin{pmatrix} \alpha(1-\mu)v\Omega(1-s,s,0) - \varepsilon v \\ -\varepsilon s \\ 0 \end{pmatrix},$$

where $\Omega(1-s,s,0)=(1-\eta)s<0$.

□

From the previous result it follows straightforwardly that

Lemma 3.2 *The tetrahedron $\mathcal{T}$ is positive invariant for the flow, i.e, if $(v_0,s_0,D_0)\in\mathcal{T}\Rightarrow\varphi(t;(v_0,s_0,D_0))\in\mathcal{T},\forall t\geq 0$, with $\varphi(t;(v_0,s_0,D_0))$ being the flow determined by system (1)-(3) and initial conditions (v_0,s_0,D_0) at time 0.*

Remark 3.3 (Growing/decreasing of the virus population) *The* nullcline *associated to v, that is $\dot{v}=0$ (for $v\neq 0$, $s\neq 0$), is given by $\alpha(1-\mu)\Omega(x)=\varepsilon$ or, equivalently, to*

$$v+\eta s+\eta_D D=\frac{\varepsilon}{\alpha(1-\mu)}.$$

There is such change in the sign of $\dot{v}$ in $\mathcal{T}$ provided that $1-\frac{\varepsilon}{\alpha(1-\mu)}\geq 0$, that is, if $\mu\leq 1-\frac{\varepsilon}{\alpha}$.

4 Equilibrium points

A crucial part on the skeleton of a dynamical system is given by its equilibrium solutions and its local behaviour around them. Such equilibria are the solutions of the system

$$\begin{aligned} &\alpha(1-\mu)v\,\Omega(x) - \varepsilon v = 0,\\ &\beta v s\,\theta(x) - \varepsilon s = 0,\\ &(\alpha\mu + \gamma D)\,v\theta(x) - \varepsilon D = 0. \end{aligned} \tag{4}$$

It is clear that the origin $(v, s, D) = (0, 0, 0)$ is a trivial equilibrium solution.

Theorem 4.1 *Our system* (1)-(3) *has three types of equilibrium points, which are of the form:*

(i) $O = (0, 0, 0)$, ***all-virus extinction****, for any value of the parameters.*

(ii) $P = (v_0, 0, D_0)$, ***virus satellite extinction****, provided that*

$$\mu < \mu_* := 1 - \frac{\varepsilon}{\alpha}. \tag{5}$$

Furthermore, v_0 *is any positive real root of the polynomial of degree* 3*:*

$$p_3(v) = A_1 v^3 + A_2 v^2 + A_3 v + A_4 = 0,$$

with

$$\begin{aligned} A_1 &= \frac{\gamma(\eta_D - 1)}{\eta_D^2},\\ A_2 &= \frac{-\mu\eta_D(\eta_D-1)(-1+\mu)\alpha^2 - 2\gamma(\eta_D-1)(-1+\mu)\alpha - \gamma\varepsilon(\eta_D-2)}{\eta_D^2\alpha(-1+\mu)},\\ A_3 &= \frac{\mu\eta_D(-1+\mu)^2(\eta_D-1)\alpha^3 + (-1+\mu)((\gamma\mu-\varepsilon-\gamma)\eta_D - \gamma(-1+\mu))\alpha^2 + \gamma\varepsilon(\eta_D-2)(-1+\mu)\alpha - \gamma\varepsilon^2}{\eta_D^2\alpha^2(-1+\mu)^2},\\ A_4 &= -\frac{\varepsilon(\alpha(-1+\mu)+\varepsilon)}{\eta_D\alpha(-1+\mu)}. \end{aligned}$$

and where

$$D_0 = \frac{1}{\eta_D}\left(1 - \frac{\varepsilon}{\alpha(1-\mu)} - v_0\right).$$

(iii) $Q = (v_1, s_1, D_1)$, ***all-virus coexistence****: necessary conditions for this kind of points to exist are* $\beta > \gamma$*,*

$$\eta_D\frac{\alpha\mu}{\beta-\gamma} + \frac{\varepsilon}{\alpha(1-\mu)} < 1, \tag{6}$$

and the existence of $v_1 = A - \eta s_1$ *with* s_1 *any root of the polynomial of degree 2:*

$$p_2(s) = (-\eta^2+\eta)s^2 + (2A\eta - A - \eta B)s + (-A^2 + AB - \frac{\varepsilon}{\beta}) = 0,$$

with

$$\begin{aligned} A &= 1-\eta_D\frac{\alpha\mu}{\beta-\gamma}-\frac{\varepsilon}{\alpha(1-\mu)}, \\ B &= 1-\frac{\alpha\mu}{\beta-\gamma}, \end{aligned}$$

where the D-component is given by

$$D_1=\frac{\alpha\mu}{\beta-\gamma}$$

and provided that $v_1+s_1+D_1\in\mathcal{T}$. Notice that from (6) it follows that

$$\eta_D\frac{\alpha\mu}{\beta-\gamma}<\frac{1}{\eta_D}<1,$$

which is equivalent to $\mu<\mu_*$, the condition of P-points to exist.

Equilibrium (i) involves, if stable, the extinction of the three virus types, and thus viral clearance. On the other hand, equilibrium (ii) involves, whenever stable, the coexistence of the standard virus with its DIPs. This equilibrium involves extinction of the virus satellite. This is positive, although not as much as in equilibrium (i).The worst case is equilibrium (iii), where the virus, the satellite and the DIP coexist all together, since the harmful medical consequences.

To ease the understanding of the proof of Theorem 4.1, we have organised it into two separate sections: 4.1 and 4.2. First, it is straightforward to check the following result.

Lemma 4.2 *One has:*

- *There are no equilibria with $v=0$ apart from the origin. This is clear since existence of virus population is necessary for satellite and DIP to exist.*
- *There are no equilibria of the form $(v,s,0)$.*

Proof.

- Let us look for equilibrium solution with $v=0$. Thus,

$$\begin{cases} \overset{(2)}{\Rightarrow} & -\varepsilon s=0 \;\Rightarrow\; s=0, \\ \overset{(3)}{\Rightarrow} & -\varepsilon D=0 \;\Rightarrow\; D=0 \end{cases}$$

  and so the solution is the origin.

- We also have to consider that there are virus and virus satellite but there is not DIP. This means $v\neq 0$, $s\neq 0$ and $D=0$. The equations take the following form:

$$\alpha(1-\mu)\,(1-v-\eta s)=\varepsilon, \tag{7}$$

$$\beta v\,(1-v-s)=\varepsilon, \tag{8}$$

$$\alpha\mu v(1-v-s)=0, \tag{9}$$

Due to (9) we have

$$1-v-s=0 \Rightarrow v+s=1 \overset{(8)}{\Rightarrow} \beta v\,(1-(v+s))0=\varepsilon,$$

contradiction since ε, the RNA degradation rate, does not vanish.

□

4.1 Proof of Theorem 4.1: no-satellite equilibrium $P=(v_0,0,D_0)$

We seek in this section equilibrium point with no-virus satellite population, this means with $v\neq 0$ and $s=0$. Since $v\neq 0$, equation (1) becomes

$$\alpha(1-\mu)\,(1-v-\eta s-\eta_D D)-\varepsilon=0.$$

As there is no satellite virus ($s=0$) we get

$$\alpha(1-\mu)\,(1-v-\eta_D D)=\varepsilon, \tag{10}$$

$$(\alpha\mu v+\gamma v D)\,(1-v-D)=\varepsilon D. \tag{11}$$

Let us assume first $D=0$. Then, equations (10) and (11) become

$$\alpha(1-\mu)\,(1-v)=\varepsilon, \tag{12}$$

$$\alpha\mu v(1-v)=0. \tag{13}$$

Due to (13) the unique possibility is that $v=1 \overset{(12)}{\Rightarrow} \varepsilon = 0$, a contradiction with the fact that $\varepsilon>0$. So we seek for an equilibrium point of the form $(v,0,D)$ with $D\neq 0$. Let us recover equations (10) and (11) and define the variable $\widetilde{x}=(v,D)$:

$$\alpha(1-\mu)\,\Omega(\widetilde{x})=\varepsilon \;\Rightarrow\; \Omega(\widetilde{x})=\frac{\varepsilon}{\alpha(1-\mu)} \tag{14}$$

$$(\alpha\mu v+\gamma v D)\,\theta(\widetilde{x})=\varepsilon D \tag{15}$$

where $\Omega(\widetilde{x})$ and $\theta(\widetilde{x})$ are $\Omega(x)$ and $\theta(x)$ assuming $s=0$. Regarding equation (14), one has that

$$\Omega(\widetilde{x})=\frac{\varepsilon}{\alpha(1-\mu)} \Leftrightarrow v+\eta_D D=1-\frac{\varepsilon}{\alpha(1-\mu)}.$$

Since v, D, and η_D are all positive, it is necessary (and sufficient) that

$$1-\frac{\varepsilon}{\alpha(1-\mu)}>0 \Leftrightarrow \alpha(-1+\mu)+\varepsilon<0 \Leftrightarrow \mu<1-\frac{\varepsilon}{\alpha} \tag{16}$$

holds. From (10) we also get

$$D = \frac{1}{\eta_D}\left(1 - \frac{\varepsilon}{\alpha(1-\mu)} - v\right). \tag{17}$$

Substituting this into equation (11) we obtain

$$p_3(v) = A_1 v^3 + A_2 v^2 + A_3 v + A_4 = 0,$$

where

$$\begin{aligned}
A_1 &= \frac{\gamma(\eta_D - 1)}{\eta_D^2}, \\
A_2 &= \frac{-\mu\eta_D(\eta_D-1)(-1+\mu)\alpha^2 - 2\gamma(\eta_D-1)(-1+\mu)\alpha - \gamma\varepsilon(\eta_D-2)}{\eta_D^2\alpha(-1+\mu)}, \\
A_3 &= \frac{\mu\eta_D(-1+\mu)^2(\eta_D-1)\alpha^3 + (-1+\mu)((\gamma\mu-\varepsilon-\gamma)\eta_D - \gamma(-1+\mu))\alpha^2 + \gamma\varepsilon(\eta_D-2)(-1+\mu)\alpha - \gamma\varepsilon^2}{\eta_D^2\alpha^2(-1+\mu)^2}, \\
A_4 &= -\frac{\varepsilon(\alpha(-1+\mu)+\varepsilon)}{\eta_D\alpha(-1+\mu)}.
\end{aligned}$$

Since $\eta_D > 1$ it follows that $A_1 > 0$. Moreover, having in mind relations (16), we have that $A_4 < 0$. Applying Descartes Rule it turns out that the polynomial of degree 3, $p_3(v)$, has at least one positive real solution v_0. From (17) one gets

$$D_0 = \frac{1}{\eta_D}\left(1 - \frac{\varepsilon}{\alpha(1-\mu)} - v_0\right),$$

for, at least, the value v_0 above. If the number of possible zeroes in the interval $(0,1)$ is either one, two or three depends strongly on the choice of the parameters. See, for instance, Figure 3 where $p_3(v)$ plotted for the choice of parameters in Table 1 and different values of μ.

α	0.3
ε	0.1
η	1.1
η_D	1.25
β	0.7
γ	0.4

Table 1: Choice of parameters.

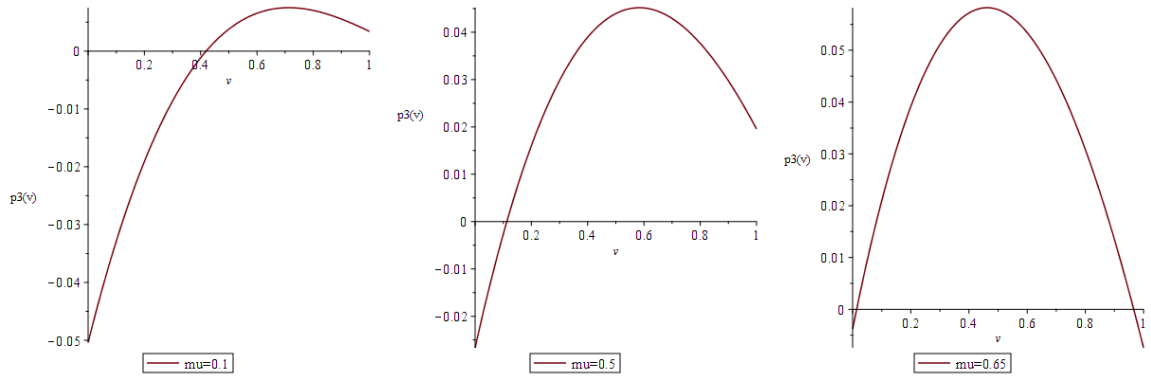

Figure 3: Plotting of the polynomial $p_3(v)$ for $v \in [0,1]$ and different values of μ. From left to right, $\mu = 0.1, 0.5$, and 0.65. Take into account that $\mu_* = 1 - (\varepsilon/\alpha) = 0.6666666$ in this case.

4.2 Proof of Theorem 4.1: coexistence equilibrium $Q = (v_1, s_1, D_1)$

This is, actually, the most interesting case, when the virus, the virus satellite, and the DIP coexist all together. This means that we assume $v \neq 0$, $s \neq 0$ and $D \neq 0$. Let us recover the system:

$$\begin{aligned} \alpha(1-\mu)v\,\Omega(x) - \varepsilon v &= 0, \\ \beta v s\,\theta(x) - \varepsilon s &= 0, \\ (\alpha\mu v + \gamma v D)\,\theta(x) - \varepsilon D &= 0. \end{aligned}$$

To study this situation, we will distinguish two cases: $\theta(x) = 0$ or $\theta(x) \neq 0$, that is, equivalently, $v + s + D = 1$ and $v + s + D < 1$, respectively. Indeed,

- $\theta(x) = 0 \Leftrightarrow v + s + D = 1$. If $\theta(x) = 0$ we get two contradictions in the last two equations of the system

$$\begin{aligned} \varepsilon s &= 0, \\ \varepsilon D &= 0, \end{aligned}$$

  since $\varepsilon \neq 0$, $s \neq 0$ and $D \neq 0$. So there are no equilibrium solutions of type Q with $\theta(x) = 0$.

- $\theta(x) \neq 0 \Leftrightarrow v + s + D < 1$ (since we restrict ourselves to the domain $\mathcal{T}$). As $v \neq 0$, $s \neq 0$ and $\theta(x) \neq 0$, we can start dividing the third equation of our system by the second one. We get

$$\frac{(\alpha\mu + \gamma D)v\theta(x)}{\beta v s \theta(x)} = \frac{\varepsilon D}{\varepsilon s} \Leftrightarrow \frac{\alpha\mu + \gamma D}{\beta s} = \frac{D}{s} \Leftrightarrow D(\beta - \gamma) = \alpha\mu \Leftrightarrow D_1 = \frac{\alpha\mu}{\beta - \gamma},$$

  and this result for D only has biological sense if $\beta > \gamma$, this is, satellite replication rate must be greater than the DIPs creation rate.

To find v and s we replace the found value of D in the system. The first two equations become

$$\alpha(1-\mu)v\,\widetilde{\Omega}(x) - \varepsilon v = 0,$$
$$\beta v s\,\widetilde{\theta}(x) - \varepsilon s = 0,$$

where $\widetilde{\Omega}(x) = 1 - v - \eta s - \eta_D \frac{\alpha\mu}{\beta-\gamma}$ and $\widetilde{\theta}(x) = 1 - v - s - \frac{\alpha\mu}{\beta-\gamma}$. Using again that $v \neq 0$ and $s \neq 0$ we get

$$\begin{aligned} \alpha(1-\mu)\widetilde{\Omega}(x) &= \varepsilon, \\ \beta v\widetilde{\theta}(x) &= \varepsilon, \end{aligned}$$

which imply

$$\widetilde{\Omega}(x) = \frac{\varepsilon}{\alpha(1-\mu)} \Leftrightarrow 1 - v - \eta s - \eta_D \frac{\alpha\mu}{\beta-\gamma} = \frac{\varepsilon}{\alpha(1-\mu)} \Leftrightarrow v + \eta s = A, \tag{18}$$

$$v\widetilde{\theta}(x) = \frac{\varepsilon}{\beta} \Leftrightarrow v(1 - v - s - \frac{\alpha\mu}{\beta-\gamma}) = \frac{\varepsilon}{\beta} \Leftrightarrow v(B - v - s) = \frac{\varepsilon}{\beta}, \tag{19}$$

provided we define

$$A = 1 - \eta_D \frac{\alpha\mu}{\beta-\gamma} - \frac{\varepsilon}{\alpha(1-\mu)}, \qquad B = 1 - \frac{\alpha\mu}{\beta-\gamma}. \tag{20}$$

Necessary conditions to exist such v, s is that $A > 0, B > 0$, this is,

$$\eta_D \frac{\alpha\mu}{\beta-\gamma} + \frac{\varepsilon}{\alpha(1-\mu)} < 1, \qquad \frac{\alpha\mu}{\beta-\gamma} < 1.$$

From the relation on the right hand-side, it follows that $\beta > \gamma$ and that $\mu < \frac{\beta-\gamma}{\alpha}$. Moreover, from the left hand-side expression, since both terms are positive, it turns out that (if $\beta > \gamma$),

$$\eta_D \frac{\alpha\mu}{\beta-\gamma} < 1 \Rightarrow \frac{\alpha\mu}{\beta-\gamma} < \frac{1}{\eta_D} < 1$$

and

$$\frac{\varepsilon}{\alpha(1-\mu)} < 1 \Rightarrow \mu < \mu_* = 1 - \frac{\varepsilon}{\alpha}.$$

From this second expression it follows that if Q equilibrium point exists then also a P-point exists, provided its corresponding component v_0 falls in the interval $(0, 1)$ and $v_0 + D_0 < 1$.

From equation (18) we have that $v = A - \eta s$ and substituting it in (19) we get the quadratic equation

$$p_2(s) = s^2(-\eta^2 + \eta) + s(2A\eta - A - \eta B) - A^2 + AB - \frac{\varepsilon}{\beta} = 0.$$

Solving it with MAPLE we get that the two possible values for the satellite are

$$s_\pm = \frac{2A\beta\eta - \beta B\eta - A\beta \pm \sqrt{B^2\beta^2\eta^2 - 2AB\beta^2\eta + A^2\beta^2 - 4\beta\varepsilon\eta^2 + 4\beta\varepsilon\eta}}{2\beta\eta(\eta - 1)},$$

provided the discriminant

$$B\beta\eta(B\eta - 2A) + A^2\beta + 4\varepsilon\eta(1-\eta) \geq 0,$$

and $v_\pm + s_\pm + D_1 < 1$, where $v_\pm = A - \eta s_\pm$. We have not found any simple expression on the parameters ensuring the existence of these points.

Example 4.3 *Using the parameters established in Table 1 we have* $D_1 = 0.1$. *After plotting* $\widetilde{\theta}(x)$ *and* $\widetilde{\Omega}(x)$ *to see the intersection points between them, we get the results that are shown in the left part of Fig. 4. In the right part, we impose* $v \in [0,1]$

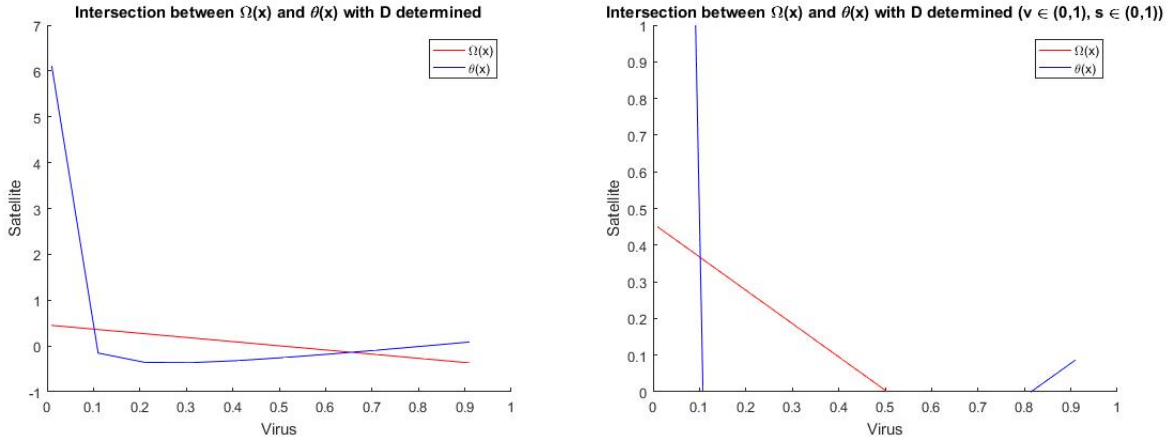

Figure 4: Plotting of $\theta(x)$ and $\Omega(x)$ after fixing all the parameters (included $\mu = 0.1$) and, as a consequence, fixing D_1. Left: intersection between $\widetilde{\Omega}(x)$ and $\widetilde{\theta}(x)$. Right: the same intersection imposing $\widetilde{\theta}(x), \widetilde{\Omega}(x) \in \mathcal{T}$.

5 Local nonlinear stability of the equilibria

Let us, before entering into the study of the stability around the equilibrium points found in the Section 4, to remind some important definitions and properties. Indeed, we consider nonlinear systems (NLS) like

$$\dot{x} = F(x)$$

where the field $F : U \to \mathbb{R}^n$ is of class C^1 in an open set $U \subset \mathbb{R}^n$. Remember that the trajectories of the system are tangent to the velocity field $F(x)$. Moreover, for each initial position there is a single orbit of the system (Picard's Theorem). Then,

Definition 5.1 *x_0 is an* equilibrium point *of the system $\dot{x} = F(x)$ when the* velocity *of the system at this point is 0, that means, $F(x_0) = 0$.*

If x_0 is an equilibrium point, the constant function $x(t) \equiv x_0$ is a solution of the nonlinear system due to

$$\dot{x}(t) = 0 = F(x_0) = F(x(t)),\ \forall t \in \mathbb{R}$$

This means that a particle that moves as a consequence of a velocity field, will be quiet when it is in a position with velocity zero. We want to know which is the behaviour of the trajectories of a nonlinear system around such kind of point. Although the next definitions are similar to the ones we have in linear systems, we must take into account some differences between them.

Definition 5.2 *Let $x_0 \in U$ be an equilibrium point of $\dot{x} = F(x)$. This point is:*

- ***Stable*** $\Leftrightarrow \forall \varepsilon > 0,\ \exists\ \delta > 0$ *such that*

$$||x(0) - x_0|| \leq \delta \Rightarrow ||x(t) - x_0|| \leq \varepsilon,\ \forall t \geq 0.$$

  Here $x(t)$ is any trajectory of the system and $x(0)$ denotes its initial condition.

- ***Unstable*** *if it is not stable.*

- ***Attractor/asymptotically stable*** $\Leftrightarrow$ *it is stable and $\exists\ \delta_0 > 0$ such that*

$$||x(0) - x_0|| \leq \delta \Rightarrow \lim_{t\to\infty} x(t) = x_0.$$

- ***Repeller*** *if and only if it is attractor for the system $\dot{x} = -F(x)$ (that is, when reversing time in our original system).*

The first difference between the linear (LSs) and the nonlinear systems (NLSs) is that while in the first case are the systems which are defined as attractors/repellers or stables/unstables, when we are working with nonlinear systems are their equilibrium points which are defined in this form. For example, a nonlinear

system can has at the same time attractor and repeller equilibrium points. Another difference between LSs and NLSs is the local character that have the definitions in nonlinear systems unlike the global character in linear ones. For example, if a LS is attractor, we can affirm that all the trajectories tend to the equilibrium point. On the other hand, if we have an attractor equilibrium point in a NLS we can only affirm that point to it the trajectories which begin sufficiently near of that point.
To study the nonlinear stability of the equilibrium points we are going to use the linearization method. The main idea is to build an homogeneous linear system with constant coefficients "similar" to the nonlinear system around the equilibrium points, expecting that the dynamic behaviour of the two systems is also similar.

Definition 5.3 *If we have the ODE $\dot{x} = F(x)$ with x_0 an equilibrium point then its linearized system at x_0 is given by $\dot{y} = DF(x_0)y$, where $y = x - x_0$ and $DF(x_0)$ denotes the Jacobian matrix at x_0.*

The following theorem is a key concept to study the nonlinear stability of a dynamical system.

Theorem 5.4 *Let $\mathcal{A} = DF(x_0)$ be the Jacobian matrix of the linearized system of a NLS around an equilibrium point x_0.*

- *If there exists an eigenvalue of $\mathcal{A}$ with positive real part, then the equilibrium point is unstable.*
- *If all eigenvalues of $\mathcal{A}$ have negative/positive real part, the equilibrium point is attractor/repeller.*
- *In the rest of the cases, the linearization does not decide the stability.*

Remark 5.5 *The existence of any eigenvalue with null real part does not prevent that this method decides the stability. For example, if the associate matrix at an equilibrium point of a 2D nonlinear system has a null eigenvalue and a positive eigenvalue, then the equilibrium point is unstable.*

Theorem 5.6 (Hartman-Grobman/Linearization theorem) *If the linearized system of a nonlinear system at an equilibrium point does not have any eigenvalue with null real part, then the linear and nonlinear system are qualitatively similar (locally around the equilibrium point).*

To sum up, the theorem states that the behaviour of a dynamical system in a domain near a hyperbolic equilibrium point is qualitatively the same as the behaviour of its linearization near this equilibrium point, where hyperbolicity means that no eigenvalue of the linearization has real part equal to zero. Therefore, when dealing with such dynamical systems one can use linearization around equilibria as a first step to determine their stability. When this method does not decide, Lyapunov functions are also considered.

Let us go again to our problem. To study the stability of our system we must calculate the Jacobian matrix and evaluate it in the equilibrium points. Namely, in our case

$$J = \begin{pmatrix} \alpha(1-\mu)(1-2v-s\eta-\eta_D D)-\varepsilon & -\alpha(1-\mu)v\eta & -\alpha(1-\mu)v\eta_D \\ \beta s(1-2v-s-D) & \beta v(1-v-2s-D)-\varepsilon & -\beta vs \\ \alpha\mu(1-2v-s-D)+\gamma D(1-2v-s-D) & -\alpha\mu v-\gamma vD & \gamma v(1-v-s-2D)-\alpha\mu v-\varepsilon \end{pmatrix}.$$

We will study its eigenvalues for any type of equilibrium points. To ease the reading we have divided the study corresponding to O, P and Q in the following sections.

5.1 Nonlinear stability of the origin

Evaluating the Jacobian at the origin,

$$J_1 = J_{(0,0,0)} = \begin{pmatrix} \alpha(1-\mu)-\varepsilon & 0 & 0 \\ 0 & -\varepsilon & 0 \\ \alpha\mu & 0 & -\varepsilon \end{pmatrix}.$$

To find the eigenvalues of J_1 we need to solve the characteristic polynomial equation for λ:

$$(-\varepsilon-\lambda)(\alpha(1-\mu)-\varepsilon-\lambda)(-\varepsilon-\lambda) = (-\varepsilon-\lambda)^2(\alpha(1-\mu)-\varepsilon-\lambda) = 0.$$

Its three roots are

$$\lambda_1 = \lambda_2 = -\varepsilon, \qquad \lambda_3 = \alpha(1-\mu)-\varepsilon. \tag{21}$$

We have to check if J_1 is a diagonalizable matrix. Let us remember the next definitions:

Definition 5.7 *The algebraic multiplicity of an eigenvalue λ_i is its multiplicity as a root of the characteristic polynomial, that is, the largest integer k such that $(\lambda - \lambda_i)^k$ divides evenly that polynomial.*

Definition 5.8 *The geometric multiplicity of an eigenvalue λ_i of a matrix $\mathcal{A}$ is the dimension of its corresponding eigenspace* $\ker(\mathcal{A} - \lambda_i Id)$ *and it is the number of Jordan blocks corresponding to λ_i.*

Definition 5.9 *$\mathcal{A}$ is a diagonalizable matrix if the algebraic and geometric multiplicities of all the eigenvalues coincide.*

Let us study the multiplicities of $\lambda = -\varepsilon$. Easily, we see that the geometric multiplicity of this eigenvalue, that is the dimension of $\ker(J_1 - (-\varepsilon)Id)$ is 2, as its algebraic multiplicity:

$$\dim(\ker(J_1 + \varepsilon Id)) = \begin{pmatrix} \alpha(1-\mu) & 0 & 0 \\ 0 & 0 & 0 \\ \alpha\mu & 0 & 0 \end{pmatrix} = 2.$$

So we can conclude that J_1 is diagonalizable and its diagonal matrix is

$$D_1 = \begin{pmatrix} \alpha(1-\mu) & 0 & 0 \\ 0 & -\varepsilon & 0 \\ 0 & 0 & -\varepsilon \end{pmatrix}.$$

Besides that, the sign of λ_3 will determine the linear and nonlinear local stability of the origin. In fact,

$$\lambda_3 < 0 \Leftrightarrow \alpha(1-\mu) < \varepsilon \Leftrightarrow \alpha < \frac{\varepsilon}{1-\mu} \Leftrightarrow 1-\mu < \frac{\varepsilon}{\alpha} \Leftrightarrow \mu > \mu_*$$

$$\lambda_3 > 0 \Leftrightarrow \alpha(1-\mu) > \varepsilon \Leftrightarrow \alpha > \frac{\varepsilon}{1-\mu} \Leftrightarrow 1-\mu < \frac{\varepsilon}{\alpha} \Leftrightarrow \mu < \mu_*$$

where remember that $\mu_* = 1 - \frac{\varepsilon}{\alpha}$ (see Theorem 4.1(ii)). This means that the origin is unstable if $\mu < \mu_*$ and becomes asymptotically stable (attractor) when $\mu > \mu_*$, coinciding with the disappearance of all the equilibrium points of P-type (if they exist). Moreover, when it is unstable, it is of node type, with an unstable invariant manifold of dimension 1.
We can see a schematic representation in Fig. 5 with the parameters established in Table 1.

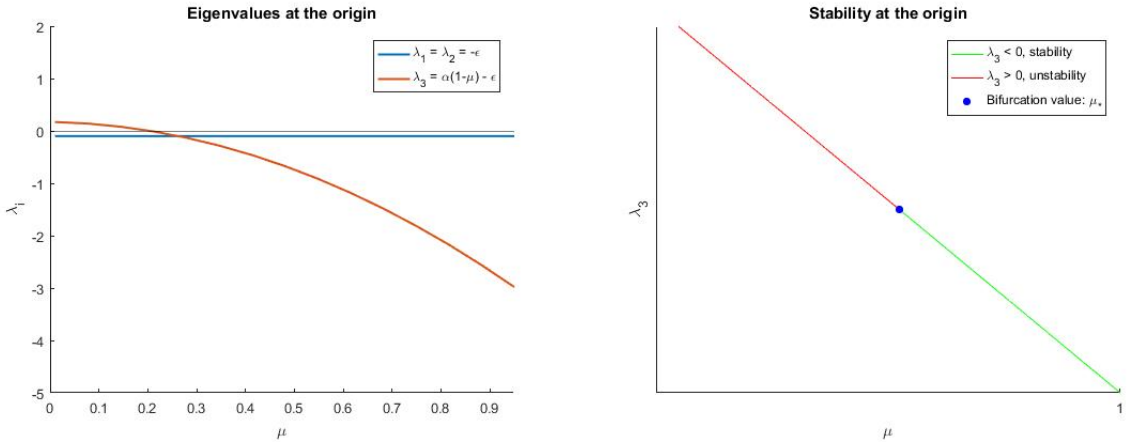

Figure 5: Left: Evolution of the eigenvalues of J_1 taking the parameters in table 1 and ranging μ from 0.01 to 0.95. Right: Representation of the stability of the origin depending on λ_3's sign.

From here we will assume $\alpha > \varepsilon$. It is reasonable to suppose that because α and ε are the replication and the degradation rate of the virus, respectively. If $\alpha < \varepsilon$ then the origin is an attractor node and, locally, it implies extinction. With other words, if $1 - \frac{\varepsilon}{\alpha}$ is negative, then the condition $\mu > 1 - \frac{\varepsilon}{\alpha}$ is trivially satisfied and we are always in the right part of Fig. 6 and this means that the stability of the origin does not undergo any bifurcation.
To sum up, if $\mu \in (0, \mu_*)$ then P exists (in principle) and the origin is unstable: it has an unstable invariant curve and O is repeller. On the other hand, if $\mu > \mu_*$ P-points (if they exist) disappear and the origin becomes attractor (asymptotically stable), of node type. This means that in μ_* exists a transcritical bifurcation.

Remark 5.10 *A* transcritical bifurcation *is a particular kind of local bifurcation, meaning that it is characterized by an equilibrium having an eigenvalue whose real part passes through zero. A transcritical bifurcation is one in which a fixed point exists for all values of a parameter and is never destroyed. However,*

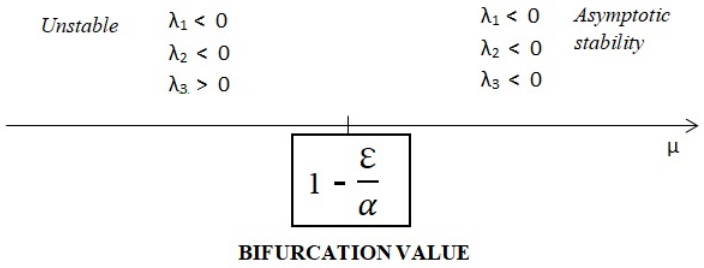

Figure 6: Bifurcation diagram of the local stability of the origin.

such a fixed point interchanges its stability with another fixed point as the parameter is varied. In other words, both before and after the bifurcation, there is one unstable and one stable fixed point. However, their stability is exchanged when they collide. So the unstable fixed point becomes stable and viceversa. The normal form of a transcritical bifurcation is

$$\frac{dx}{dt} = rx - x^2,$$

which is similar to the logistic equation (see remark 2.1).

At this point we can seek for the eigenvectors of J_1. If we focus on the second and third columns of the matrix J_1, we find

$$\lambda_1 = -\varepsilon \longrightarrow v_1 = (0, 1, 0),$$
$$\lambda_2 = -\varepsilon \longrightarrow v_2 = (0, 0, 1).$$

Solving $\ker(J_1 - \lambda_3 Id)$ we obtain

$$\lambda_3 = \alpha(1-\mu) - \varepsilon \longrightarrow v_3 = \left(\frac{1-\mu}{\mu}, 0, 1\right).$$

As $0 < \mu \ll 1$ we conclude that the first component of v_3 is positive.

At the origin, the local stable manifold is tangent to the plane $v = 0$ because we know that the local stable and unstable manifolds of the nonlinear system are tangents, in the equilibrium point, to the stable and the unstable manifolds of the linear system, respectively.

5.2 Nonlinear stability at equilibria of type $P = (v_0, 0, D_0)$

Here we are going to proceed as in the previous section. Evaluating the Jacobian matrix at $(v, 0, D)$ we get:

$$J_2 = J_{(v,0,D)} = \begin{pmatrix} \alpha(1-\mu)(1-2v-\eta_D D) - \varepsilon & -\alpha(1-\mu)v\eta & -\alpha(1-\mu)v\eta_D \\ 0 & \beta v(1-v-D) - \varepsilon & 0 \\ \alpha\mu(1-2v-D) + \gamma D(1-2v-D) & -\alpha\mu v - \gamma v D & \gamma v(1-v-2D) - \alpha\mu v - \varepsilon \end{pmatrix}.$$

We recover (17) from section 4.1:

$$D = (1 - \frac{\varepsilon}{\alpha(1-\mu)} - v)\frac{1}{\eta_D}.$$

This value for D has only biological sense if $1 - \frac{\varepsilon}{\alpha(1-\mu)} > v$. So the necessary condition of the existence of the equilibrium point P is $v < 1 - \frac{\varepsilon}{\alpha(1-\mu)}$. In particular, $1 - \frac{\varepsilon}{\alpha(1-\mu)} > 0$ which means $\mu < \mu_*$, the condition of P to exist.

To study the stability of P we have to calculate the eigenvalues of J_2. Using MAPLE we get an easy expression for one of the eigenvalues:

$$\lambda_1 = -v(D + v - 1)\beta - \varepsilon,$$

while the other two will require a numerical approach. As $(v, s, D) \in \{\theta(x) > 0\} \Leftrightarrow v + s + D < 1$, imposing $s = 0$ we can conclude

$$0 < v + D < 1 \Leftrightarrow D + v - 1 < 0 \Leftrightarrow -v\beta(D + v - 1) = v\beta(1 - v - D) = -v(D + v - 1)\beta > 0$$

So, therefore,

Lemma 5.11 *If $v(1 - v - D) > \varepsilon/\beta$ then $\lambda_1 > 0$ and, consequently, P is unstable.*

To study the stability of P we have fixed all parameters except from μ, the parameter governing the growth of DIPs from the virus. As we have seen in section 4.1, v_0 is any real solution in $(0, 1)$ of the third degree polynomial

$$p_3(v) = A_1 v^3 + A_2 v^2 + A_3 v + A_4 = 0.$$

Figure 7 represents $p_3(v)$ for the choice of parameters in Table 2 and three different values of μ from 0 to μ_*.

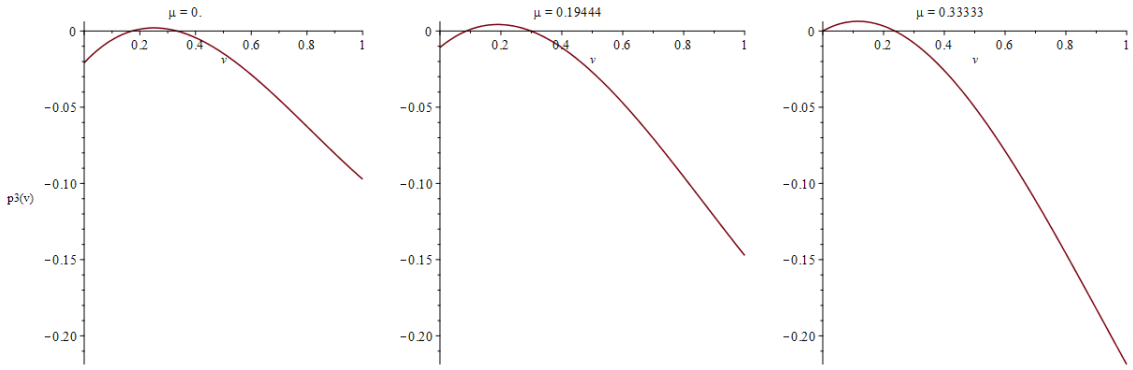

Figure 7: Plotting of the polynomial $p_3(v)$ for $v \in [0,1]$ and, from left to right, $\mu = 0, \mu = 0.1.9444$ and $\mu_* = 0.3333$ for the choice of parameters in Table 2.

α	0.15
ε	0.1
η	1.35
η_D	1.6
β	0.63
γ	0.8

Table 2: Choice of parameters

Once calculated the third degree polynomial $p_v(\mu)$ depending on v and μ we have found its roots. In Fig. 8 we can see the evolution of the three solutions in terms of μ.
If we focus on the plot we can see that we have three real solutions. Despite that, we are not interested in the green one because it is greater than 1 and as we are in $v + s + D \leq 1$ we want $v < 1$. The plot of the imaginary part of the solutions confirm that the solutions are real because they are of order 10^{-19}, which is negligible.

For each of the effective equilibrium points above we determine its linear stability depending if the solutions are real or not.

- **Red solution:** v_1.
  It has biologically sense while it is positive, something that happens until $\mu \approx 0.36$. Once we have fixed the solution we have calculated the Jacobian matrix J_2 of the system with v_{01} and D_{01} fixed. We have found the three eigenvalues of J_2 (λ_1, λ_2 and λ_3, respectively) and we have plotted their real and imaginary parts, as we can see in Fig. 9.

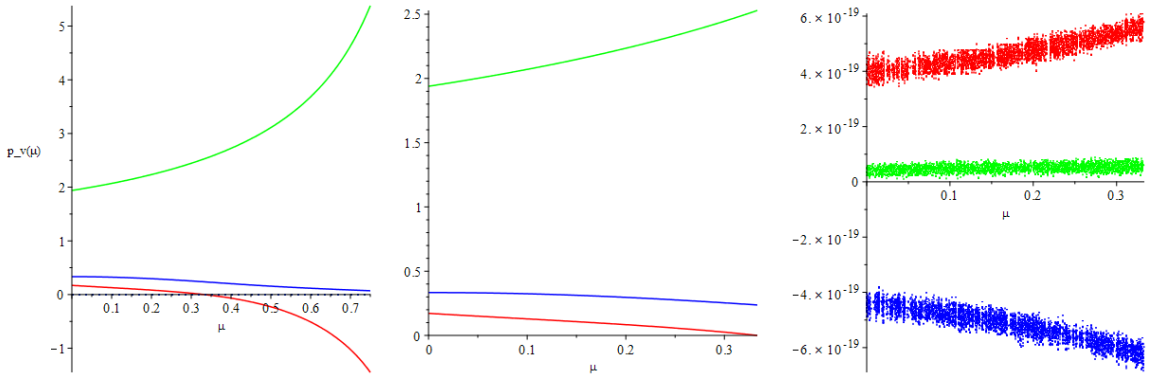

Figure 8: Plotting of the evolution of the solutions of polynomial $p_v(\mu)$ for $\mu \in [0, \mu_*]$. From left to right: the solutions, their real part and imaginary one, respectively.

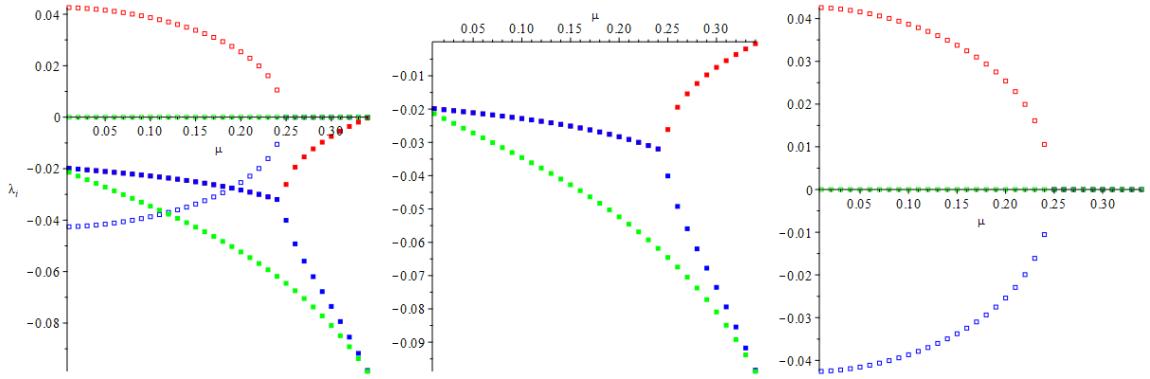

Figure 9: Plotting of the eigenvalues of $P = (v_{01}, 0, D_{01})$ related to J_2. Real parts in solid boxes and imaginary parts in empty ones.

While λ_3 (green) is always real and negative, λ_1 (red) and λ_2 (blue) are complex (and conjugates), with negative real part up to $\mu \approx \widetilde{\mu} = 0.25$. Then, up to $\mu = \mu_* = 1 - \frac{\varepsilon}{\alpha}$, they become real and negative. While λ_2 tends to -0.09, λ_1 tends to 0 when μ reaches μ_*. Therefore, up to $\widetilde{\mu}$ we have that P is an attractor focus $\times$ attractor node, which means attractor (asymptotically stable). One has attracting spiral behaviour nearby. On the other hand, for $\mu > \widetilde{\mu}$ we have an attractor node. In $\widetilde{\mu}$ we have a bifurcation in the point type but the stability does not change, P continues being an attractor.

- **Green solution:** v_2.
  We discard this solution since it is not in $v + s + D \leq 1$.

- **Blue solution:** v_3.
  It is positive for all $\mu \in (0, \mu_*)$. Working like in the red solution, the eigenvalues of J_2 related to v_{03} and D_{03} are plotted in Figure 10. In this case, the three eigenvalues (λ_1, λ_2 and λ_3) are

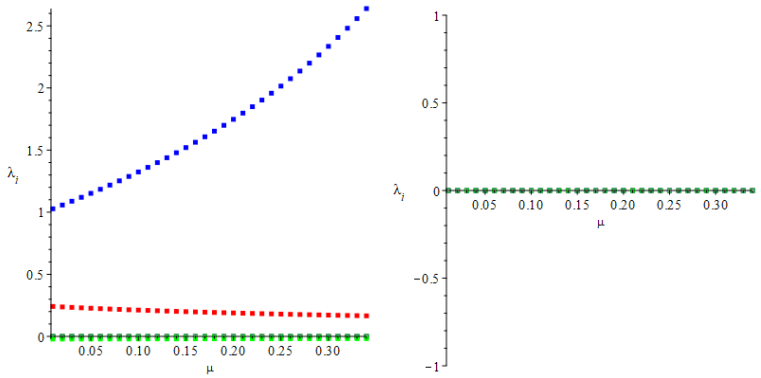

Figure 10: Plotting of the eigenvalues of $P = (v_{03}, 0, D_{03})$ related to J_2. Real parts in solid boxes and imaginary parts in empty ones.

real: two of them are always positive and the other one is always zero. This means that, for the linearized system, $P = (v_{03}, 0, D_{03})$ is an unstable node (in particular, a degenerate node because one eigenvalue is 0), with a linear unstable manifold of dimension 2 and a linear neutral invariant manifold of dimension 1. For the nonlinear system, the corresponding point P_3 is unstable, with an unstable manifold with dimension, at least, 2. Despite that, in this case we can not affirm if the null eigenvalue will has an attractor or a repeller behaviour.

5.2.1 Behaviour of P points at the bifurcation value $\mu = \mu_*$

Let us consider P at the bifurcation value $\mu = \mu_*$. Working like in section 4.1 and taking $\mu = \mu_*$ we get

$$D_0 = \frac{1}{\eta_D}\left(1 - \frac{\varepsilon}{\alpha(1-\mu_*)} - v\right) = -\frac{v}{\eta_D},$$

that is negative except for the case $v = 0$, which is, precisely, solution of the third degree polynomial

$$p_3(v) = A_1 v^3 + A_2 v^2 + A_3 v = 0,$$

where

$$\begin{aligned} A_1 &= \frac{\gamma(\eta_D - 1)}{\eta_D^2}, \\ A_2 &= \frac{(-\alpha + \varepsilon)\eta_D + \alpha - \gamma - \varepsilon}{\eta_D}, \\ A_3 &= \frac{(\alpha - \varepsilon)\eta_D + \varepsilon}{\eta_D}. \end{aligned}$$

This means that the unique solution is $v = D = 0$.

Lemma 5.12 *When $\mu = \mu_*$, P-points collide and become the origin, that means, P tends to O as $\mu \to \mu_*^-$.*

5.2.2 Nonlinear stability at equilibria of type $P = (v_0, 0, D_0)$, varying α

We refine the study fixing the same parameters as before, but also considering the value of α. We have chosen the viral replication rate as the parameter to take into account since, fixed ε, α determines the interval of μ such that P exists.
As in section 5.2, we look for the real solutions $v_0 \in (0, 1)$ of the third degree polynomial

$$p_3(v) = A_1 v^3 + A_2 v^2 + A_3 v + A_4 = 0.$$

Since the $v_0 + D_0 \leq 1$ we will discard, in principle, those solutions v which are not in the interval $(0, 1)$. We have chosen some values for α.

- Case $\alpha = 0.05$.
  Figure 11 represents $p_3(v)$ for the choice of parameters in Table 3 and three different values of μ from 0 to $\mu_* = 1 - \varepsilon/\alpha$.

ε	0.01
η	1.35
η_D	1.6
β	0.63
γ	0.8

Table 3: Choice of parameters for $\alpha = 0.05$

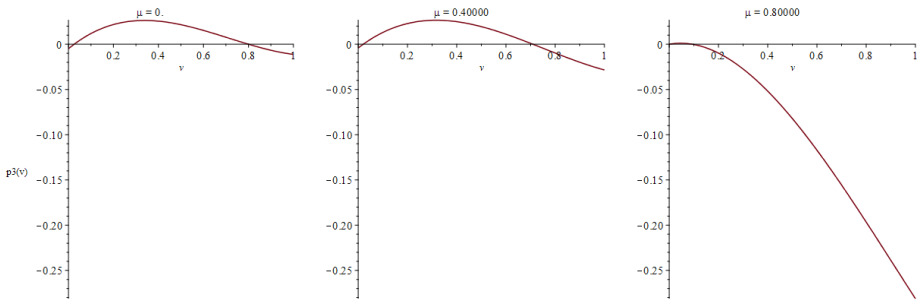

Figure 11: Plotting of the polynomial $p_3(v)$ for $v \in [0, 1]$ and $\mu = 0, \mu = 0.4$ and $\mu = 0.8$, respectively.

Fig. 12 represents the evolution of the three (real) solutions of the polynomial in terms of μ from 0 to μ_*. Indeed, the plot of the imaginary part of the solutions (see Fig. 12) is a numerical evidence

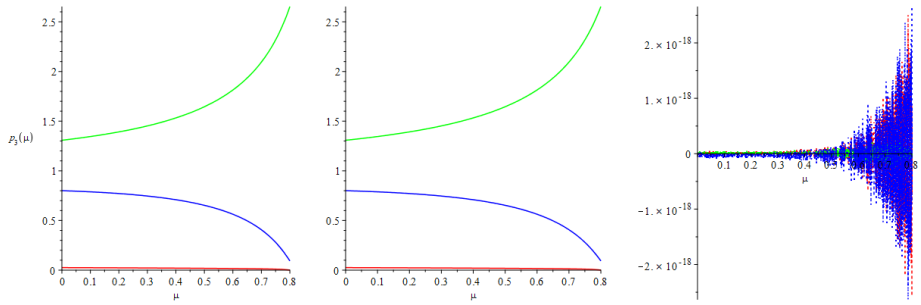

Figure 12: Plotting of the evolution of the solutions of polynomial $p_v(\mu)$ for $\mu \in [0, \mu_*]$. From left to right: the solutions, their real part and imaginary one, respectively.

that the solutions are real since they are of order 10^{-18}, which can be negligible. We also neglect the green one because it is greater than 1. For each one of the other two equilibrium points we compute the eigenvalues of their Jacobian matrix.

– **Red solution:** v_1.
Their eigenvalues λ_1, λ_2 and λ_3 (with their real and imaginary parts) are plotted in Fig. 13. Observe that λ_3 (green) is real negative and λ_1 (red), λ_2 (blue) are complex (conjugate). So $P = (v_{01}, 0, D_{01})$ is an attractor focus $\times$ stable node, that is, attractor (asymptotically stable).

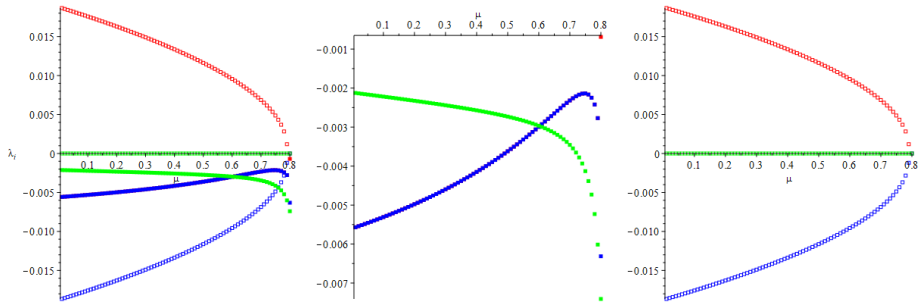

Figure 13: Eigenvalues of J_2 corresponding to $P = (v_{01}, 0, D_{01})$. Real parts in solid boxes and imaginary parts in empty ones. Left: all together; middle: real parts; right: imaginary parts.

– **Blue solution:** v_3
Fig. 14 represents the three eigenvalues of the Jacobian matrix J_2 at the point $P = (v_{03}, 0, D_{03})$. In this case, all three, λ_1, λ_2 and λ_3, are real: two of them are always positive and the other one is always zero. This means that, for the linearized system, $P = (v_{03}, 0, D_{03})$ is an unstable node (degenerate, since its determinant vanishes) with a lineal unstable manifold of dimension

2 and a lineal neutral manifold of dimension 1. For the corresponding nonlinear system we can ensure that it is also unstable with an unstable invariant manifold of dimension, at least, 2.

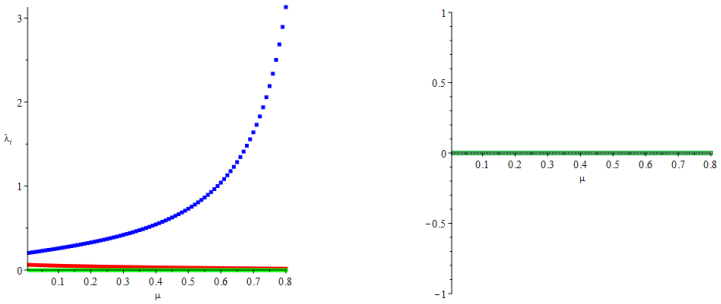

Figure 14: Plotting of the eigenvalues of J_2 related to $P = (v_{03}, 0, D_{03})$ for $\alpha = 0.05$. Real parts in solid boxes (left) and imaginary parts in empty ones (right).

- Case $\alpha = 0.5$.
  Fig. 15 represents $p_3(v)$ for the choice of parameters in Table 4 and three different values of μ from 0 to μ_*.

ε	0.1
η	1.35
η_D	1.6
β	0.7525
γ	1.15

Table 4: Choice of parameters for $\alpha = 0.5$

The three solutions of $p_3(v)$ when $\alpha = 0.5$ are represented in Fig. 16. We are only considering the red solution (which is always real).

– **Red solution:** v_1.
  Its eigenvalues are represented in figure 17. Notice that up to $\mu \approx 0.77$ λ_1 (red) and λ_2 (blue) are complex conjugates with negative real part and λ_3 is real negative. Therefore, P is an attractor focus × attractor node, which is asymptotically stable.

  From this value of $\mu \approx 0.77$ to μ_*, the two complex conjugate eigenvalues seem to collide and become real negative. A more accurate numerical analysis should be done. If that was the case, it would become an stable node (and, therefore, asymptotically stable).

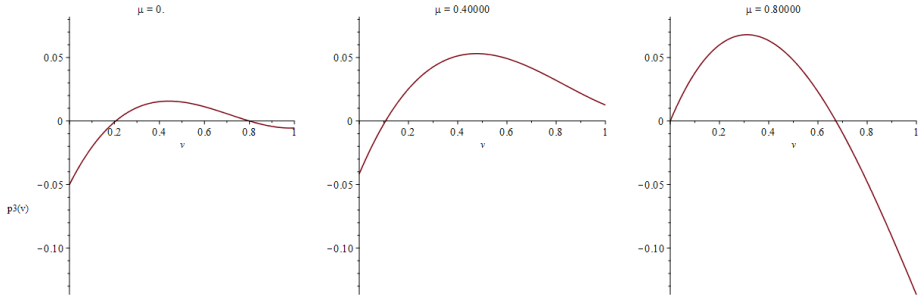

Figure 15: Plotting of the polynomial $p_3(v)$ for $v \in [0,1]$, $\alpha = 0.5$ and $\mu = 0, \mu = 0.4$ and $\mu = 0.8$, respectively.

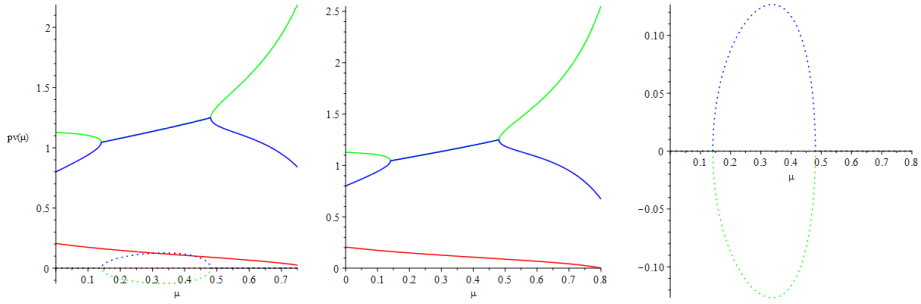

Figure 16: Plotting of the solutions of polynomial $p_v(\mu)$ for $\mu \in [0, \mu_*]$. From left to right: the solutions (real and imaginary parts), their real part and their imaginary part, respectively.

- $\alpha = 0.95$.
  Fig. 18 represents $p_3(v)$ for the choice of parameters in Table 5 and three different values of μ from 0 to μ_*.

ε	0.1
η	1.35
η_D	1.6
β	0.91
γ	1.6

Table 5: Choice of parameters for $\alpha = 0.95$

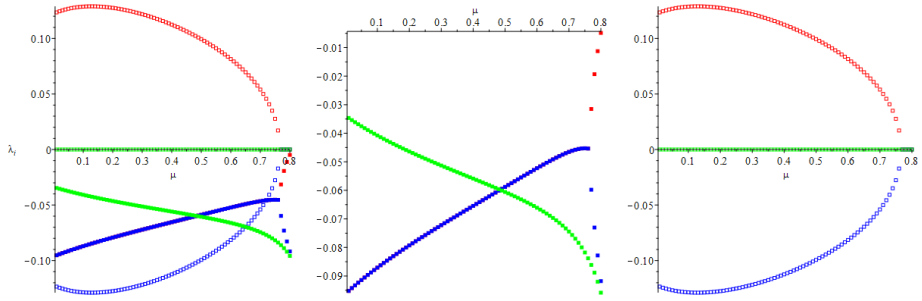

Figure 17: Plotting of the eigenvalues of the jacobian matrix at the point $P = (v_{01}, 0, D_{01})$ for $\alpha = 0.5$. Real parts in solid boxes and imaginary parts in empty ones. From left to right: real and imaginary parts of each eigenvalue, only real parts, and only imaginary ones.

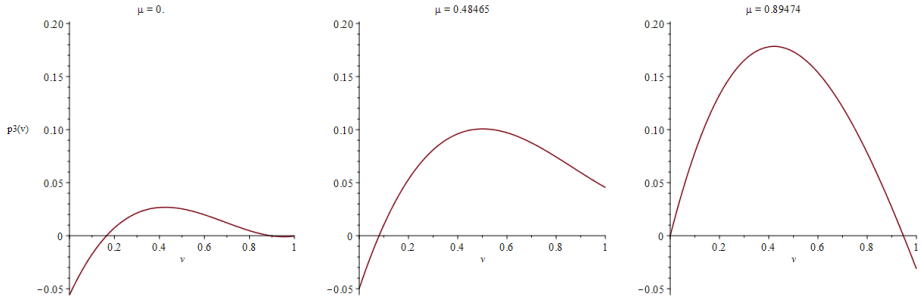

Figure 18: Plotting of the polynomial $p_3(v)$ for $v \in [0, 1]$ and $\mu = 0, \mu = 0.48465$ and $\mu_* = 0.8974$, respectively.

The three solutions of $p_3(v)$ when $\alpha = 0.95$ are represented in Fig. 19.

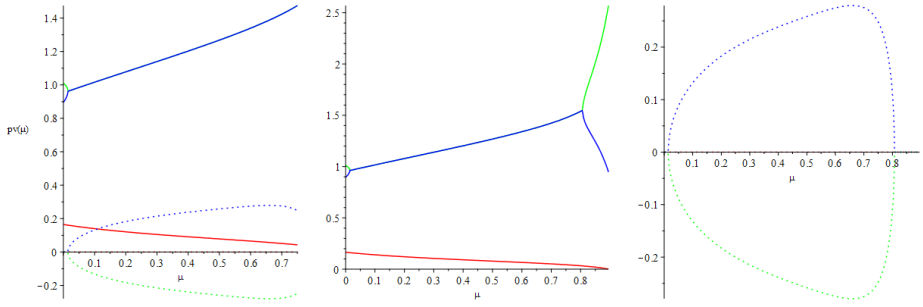

Figure 19: Plotting of the solutions of polynomial $p_v(\mu)$ for $\mu \in [0, \mu_*]$. From left to right: the solutions, their real part and the imaginary one, respectively.

We are only interested in the red solution. Concerning the stability of its associated equilibrium point:

- **Red solution**: v_1

  Fig. 20 represents the eigenvalues of J_2 at the equilibrium point $P = (v_{01}, 0, D_{01})$. While λ_3 (green) is always real and negative, λ_1 (red) and λ_2 (blue) are, up to $\mu \approx 0.88$, complex and conjugate, with negative real part. This means that we have an attractor node $\times$ attractor focus. From $\mu \approx 0.88$ it seems that the pair of complex eigenvalues collide and become real negative. If that was the case the point would become of stable node type and, therefore, asymptotically stable. A more accurate study to this region is required.

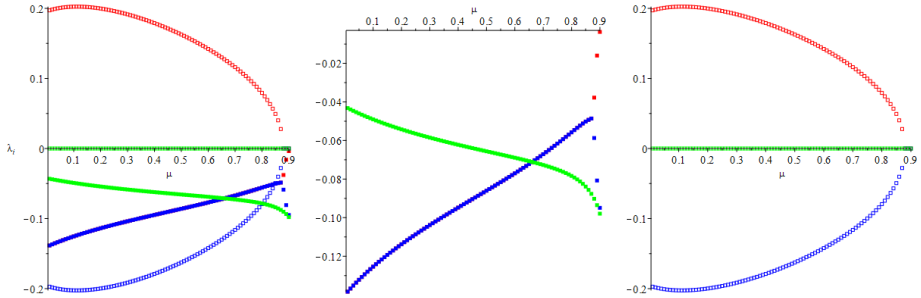

Figure 20: Plotting of the eigenvalues of the jacobian matrix J_2 at the point $P = (v_{01}, 0, D_{01})$ for $\alpha = 0.95$. Real parts in solid boxes and imaginary parts in empty ones. From left to right: real and imaginary parts of each eigenvalue, only real parts, and only imaginary ones.

5.3 Nonlinear stability at $Q = (v_1, s_1, D_1)$

Recovering the general case we get the Jacobian matrix:

$$J_3 = J_{(v,s,D)} = \begin{pmatrix} \alpha(1-\mu)(1-2v-s\eta-\eta_D D)-\varepsilon & -\alpha(1-\mu)v\eta & -\alpha(1-\mu)v\eta_D \\ \beta s(1-2v-s-D) & \beta v(1-v-2s-D)-\varepsilon & -\beta vs \\ \alpha\mu(1-2v-s-D)+\gamma D(1-2v-s-D) & -\alpha\mu v-\gamma vD & \gamma v(1-v-s-2D)-\alpha\mu v-\varepsilon \end{pmatrix}$$

From section 4.2, as $v, s, D \neq 0$ we have

$$D = \frac{\alpha\mu}{\beta-\gamma}.$$

Remember that this value of D has only biological sense if $\beta > \gamma$. Let us recover the equations with which we are going to work in this section:

$$v + \eta s = A, \qquad v(B - v - s) = \frac{\varepsilon}{\beta},$$

where $A = 1 - \eta_D D - \frac{\varepsilon}{\alpha(1-\mu)}$ and $B = 1 - D$. Moreover, necessary condition for the existence of Q is that

$$\mu < \min\left\{\mu_*, \frac{\beta-\gamma}{\alpha\eta_D}\right\}.$$

To study the stability of Q we have fixed all parameters except from μ. As we have seen in section 4.2, s_0 is the solution of the second degree polynomial

$$p_2(s) = s^2(-\eta^2 + \eta) + s(2A\eta - A - \eta B) - A^2 + AB - \frac{\varepsilon}{\beta} = 0.$$

Figure 21 represents $p_2(s)$ for the choice of parameters in Table 6 and three different values of μ from 0 to $\widetilde{\mu} = \min\left\{\mu_*, \frac{\beta-\gamma}{\alpha\eta_D}\right\}$.

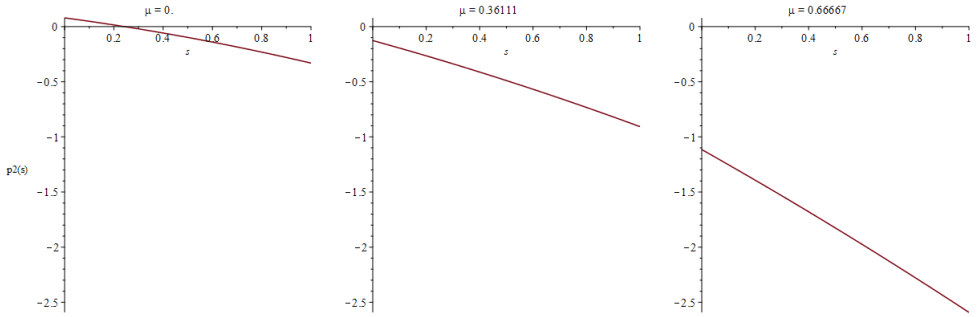

Figure 21: Plotting of the polynomial $p_2(s)$ for $s \in$ [0,1] and, from left to right, $\mu = 0, \mu = 0.3611$ and $\widetilde{\mu} = 0.6667$.

α	0.3
ε	0.1
η	1.1
η_D	1.25
β	0.7
γ	0.4

Table 6: Choice of parameters

Once calculated the second degree polynomial $p_s(\mu)$ depending on s and μ we have found its roots. In Figure 22 we can see the evolution of the two solutions in terms of μ.
The two solutions are real. Despite that, we are not interested in the one which is represented in red because it is negative and as we are in $v + s + D \leq 1$ we want $s \in (0, 1)$.

So we have to determine the linear stability of the solutions.

- **Green solution:** s_2.
  Once we have fixed the solution we have calculated the Jacobian matrix J_2 of the system with v_{12},

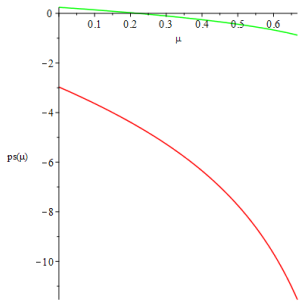

Figure 22: Plotting of the evolution of the solutions of polynomial $p_s(\mu)$ for $\mu \in [0, \widetilde{\mu}]$.

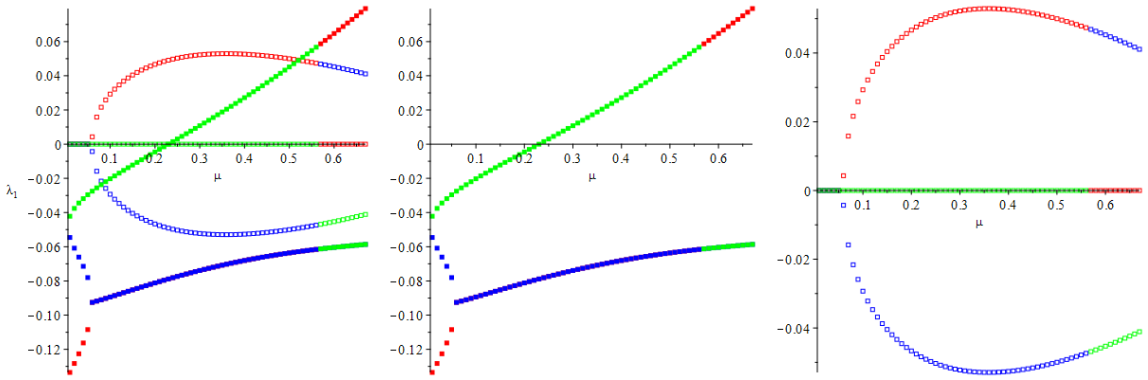

Figure 23: Eigenvalues of J at the point $Q = (v_{12}, s_{12}, D_{12})$. Real parts in solid boxes and imaginary parts in empty ones. From left to right: real and imaginary parts of each eigenvalue, only real parts, and only imaginary ones. The changes of colour come from the way that Maple order, and therefore plot, the eigenvalues it founds.

s_{12}, and D_{12} fixed. We have found the three eigenvalues of J_2 (λ_1, λ_2 and λ_3, respectively) and we have plotted their real and imaginary parts, as we can see in Figure 23.

Observe that up to $\hat{\mu} \approx 0.23$ we have that λ_1 and λ_2 are complex (conjugate) with negative real part and λ_3 is real negative, so we have that Q is an stable focus $\times$ stable node. On the other hand, from $\hat{\mu}$, the real eigenvalue becomes positive real. So Q is of stable focus $\times$ unstable node type and so it is unstable. $\mu = \hat{\mu}$ is a bifurcation value.
Moreover, $\mu = \hat{\mu}$ is a bifurcation value in $P = (v_{01}, 0, D_{01})$ that changes its stability.

5.3.1 Nonlinear stability at equilibria of type $Q = (v_1, s_1, D_1)$, varying α

As we have done in section 5.2.2, we take into account the value of α to determine the stability of Q-points. As in section 5.3, we look for the real solutions s_0 in $(0, 1)$ of the second degree polynomial

$$p_2(s) = s^2(-\eta^2 + \eta) + s(2A\eta - A - \eta B) - A^2 + AB - \frac{\varepsilon}{\beta}.$$

We use three different values for α: α near 0, $\alpha = 0.5$ and α near 1.

- Case $\alpha = 0.05$.

  Figure 24 represents $p_2(s)$ for the choice of parameters in Table 7 and three different values of μ from 0 to $\widetilde{\mu} = \min\left\{\mu_*, \frac{\beta-\gamma}{\alpha\eta_D}\right\}$.

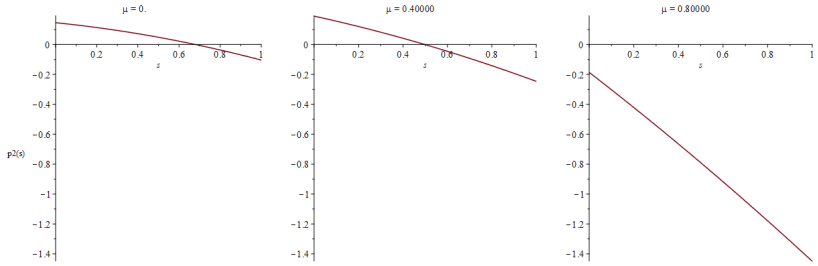

Figure 24: Plotting of the polynomial $p_2(s)$ for $s \in$ [0,1] and, from left to right, $\mu = 0, \mu = 0.4$ and $\widetilde{\mu} = 0.8$.

ε	0.01
η	1.1
η_D	1.25
β	0.7
γ	0.4

Table 7: Choice of parameters for $\alpha = 0.05$

Once calculated the second degree polynomial $p_s(\mu)$ depending on s and μ we have found its roots. In Figure 25 we can see the evolution of the two solutions in terms of μ.

The two solutions are real but we only focus on the green solution since the red one is negative. We study the linear stability of the corresponding solutions.

- **Green solution:** s_2.
  Once we have fixed the solution we have calculated the Jacobian matrix J_2 of the system with

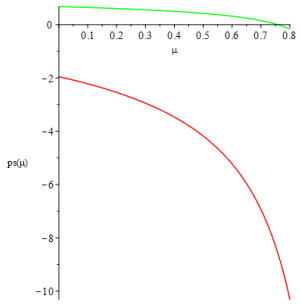

Figure 25: Plotting of the evolution of the solutions of polynomial $p_s(\mu)$ for $\mu \in [0, \widetilde{\mu}]$.

v_{12}, s_{12}, and D_{12} fixed. We have found the three eigenvalues of J_2 (λ_1, λ_2 and λ_3, respectively) and we have plotted their real and imaginary parts, as we can see in Figure 26.

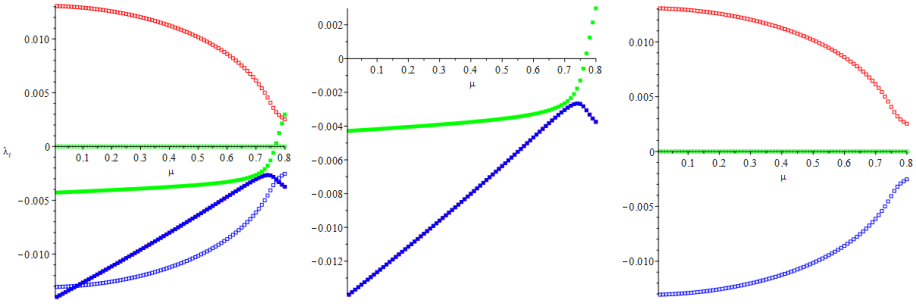

Figure 26: Plotting of the eigenvalues of J related to $Q = (v_{12}, s_{12}, D_{12})$ for $\alpha = 0.05$. Real parts in solid boxes and imaginary parts in empty ones. From left to right: real and imaginary parts of each eigenvalue, only real parts, and only imaginary ones.

Eigenvalues λ_1 (red) and λ_2 (blue) are complex and conjugates, with negative real part. On the other hand, λ_3 is negative and real up to $\mu \approx 0.77$. In this case we have that Q is an attractor. From $\mu \approx 0.77$, λ_3 is real and positive and therefore Q becomes unstable. Hence, $\mu \approx 0.77$ is a bifurcation value.
In this case, this bifurcation value does not involve any change in P-points.

- Case $\alpha = 0.5$
  In this case we have used the same parameters as in the previous one (see Table 7). Figure 27 represents $p_2(s)$ for the choice of these parameters and three different values of μ from 0 to $\widetilde{\mu} = \min\left\{\mu_*, \frac{\beta-\gamma}{\alpha\eta_D}\right\}$.

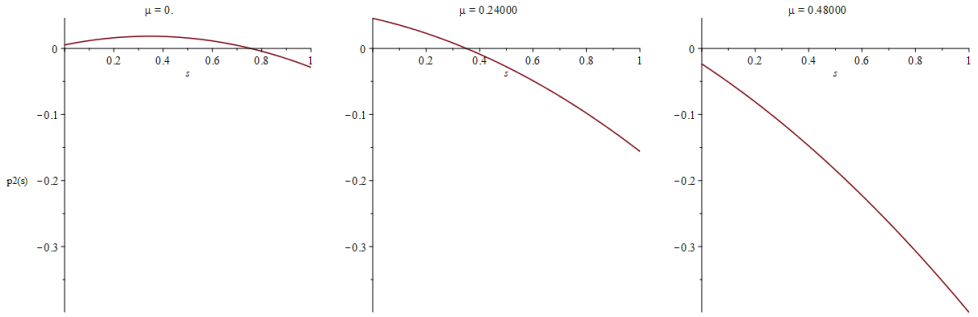

Figure 27: Plotting of the polynomial $p_2(s)$ for $s \in [0,1]$ and, from left to right, $\mu = 0, \mu = 0.24$ and $\widetilde{\mu} = 0.48$.

Again, once calculated the second degree polynomial $p_s(\mu)$ depending on s and μ we have found its roots. In Figure 28 we can see the evolution of the two solutions in terms of μ.

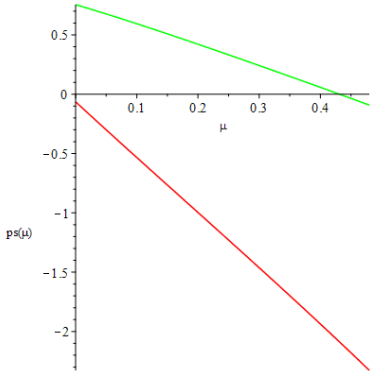

Figure 28: Plotting of the evolution of the solutions of polynomial $p_s(\mu)$ for $\mu \in [0, \widetilde{\mu}]$.

The two solutions are real, but we only focus on the green solution due to the red one is negative. We have to determine the linear stability of the solutions.

– **Green solution:** s_2.
  We are going to study the stability of $Q = (v_{12}, s_{12}, D_{12})$ depending on the eigenvalues of J (λ_1, λ_2, and λ_3) at this point. In Figure 29 we have plotted their real and imaginary parts.

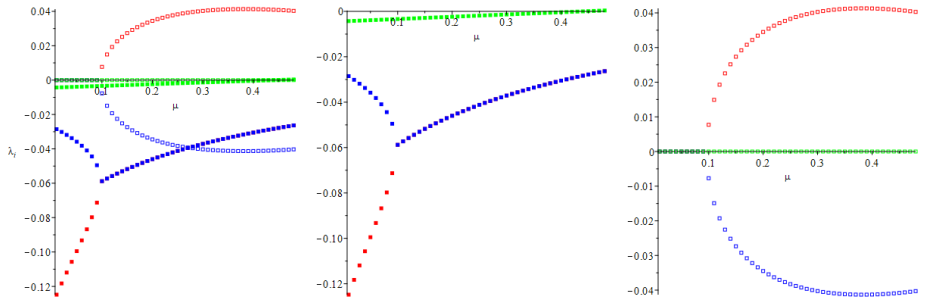

Figure 29: Plotting of the eigenvalues of J related to $Q = (v_{12}, s_{12}, D_{12})$ for $\alpha = 0.5$. Real parts in solid boxes and imaginary parts in empty ones. From left to right: real and imaginary parts of each eigenvalue, only real parts, and only imaginary ones.

λ_3 (green) is always real, but up to $\mu = \mu_2 \approx 0.45$ is negative and from this value of μ it becomes positive (this value is near μ_*). On the other hand, up to $\mu = \mu_1 \approx 0.1$ λ_1 (red) and λ_2 (blue) are real and negative.

So, summarising: for $\mu \in (0, \mu_1)$ Q is an stable node (attractor); for $\mu \in (\mu_1, \mu_2)$ it is stable focus $\times$ stable node (attractor again); and for $\mu \in (\mu_2, \mu_*)$, Q becomes of type stable focus $\times$ unstable node and, consequently, unstable. So $\mu = \mu_2$ is a bifurcation value.

- Case $\alpha = 0.95$

  In this case we have used the same parameters as in the two previous ones (see Table 7). Figure 30 represents $p_2(s)$ for the choice of these parameters and three different values of μ from 0 to $\widetilde{\mu} = \min\left\{\mu_*, \frac{\beta-\gamma}{\alpha\eta_D}\right\}$.

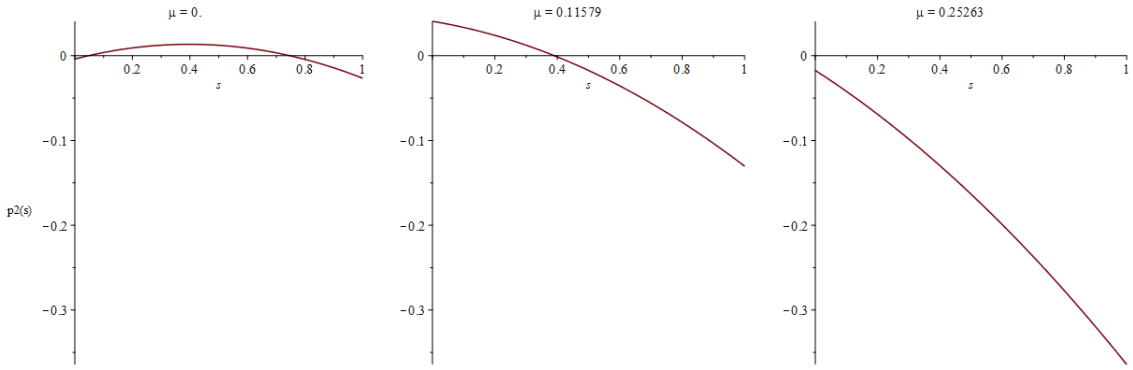

Figure 30: Plotting of the polynomial $p_2(s)$ for $s \in$ [0,1] and, from left to right, $\mu = 0, \mu = 0.11579$ and $\widetilde{\mu} = 0.25263$. If $\mu = \widetilde{\mu}$, there is not any real solution of $p_2(s)$ with $s \in [0, 1]$.

Again, once calculated the second degree polynomial $p_s(\mu)$ depending on s and μ we have found its roots. In Figure 31 we can see the evolution of the two solutions in terms of μ.

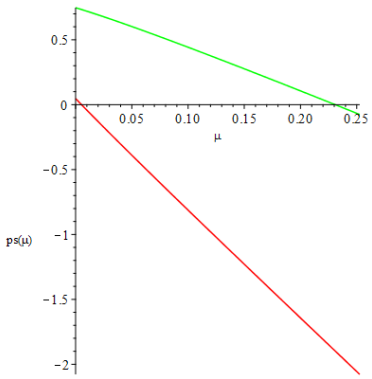

Figure 31: Plotting of the evolution of the solutions of polynomial $p_s(\mu)$ for $\mu \in [0, \widetilde{\mu}]$.

The two solutions are real but only the green one is positive (up to $\mu = \mu_2 \approx 0.23$).

– **Green solution:** s_2.
  In Fig. 32 we have plotted the eigenvalues of the Jacobian at the corresponding equilibrium point.

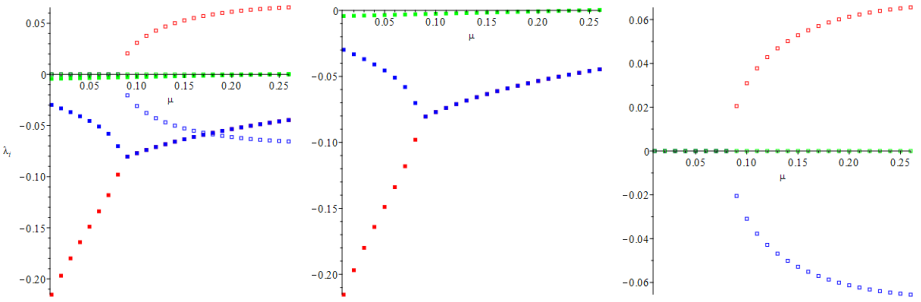

Figure 32: Plotting of the eigenvalues of J related to $Q = (v_{12}, s_{12}, D_{12})$ for $\alpha = 0.95$. Real parts in solid boxes and imaginary parts in empty ones. From left to right: real and imaginary parts of each eigenvalue, only real parts, and only imaginary ones.

λ_3 (green) is real and negative up to $\mu = \mu_2$ and afterwards it becomes positive. Up to $\mu = \mu_1 \approx 0.08$, λ_1 (red) and λ_2 (blue) are negative, real and different. From this value on they become complex (conjugate) with negative real part.

So, for $\mu \in (0, \mu_1)$, Q is an stable node (attractor) and for $\mu \in (\mu_1, \mu_2)$ it becomes of stable focus $\times$ stable node and, so attractor again. There is no change in the stability at $\mu = \mu_1$ but yes in their local configuration.

6 Long-time dynamics and dynamics on the border of $\mathcal{T}$

From Lemma 3.2 it is natural to consider the study of the dynamics restricted to the tetrahedron $\mathcal{T}$. This section is devoted to the *global* dynamics on $\mathcal{T}$ and, more precisely, onto its border. First of all we study the dynamics on the coordinate axes.

Lemma 6.1 *The vector field points, on v-axis, towards the tetrahedron $\mathcal{T}$ (except inside it where the dynamics points to $\frac{\varepsilon}{\alpha(1-\mu)}$) and makes invariant s, D-axes.*

Proof.

- **Dynamics on v-axis.**

  Choosing a point on the v-axis, that is $(v, 0, 0)$, and substituting it in our system (1)-(3), we get:

$$\dot{v} = (\alpha(1-\mu)(1-v) - \varepsilon)v, \tag{22}$$
$$\dot{s} = 0, \tag{23}$$
$$\dot{D} = \alpha\mu v(1-v). \tag{24}$$

  We are going to distinguish between $v > 1$, $v < 1$ or $v = 1$.

  - If we are outside the tetrahedron ($v > 1$) then $v + s + D > 1 \Rightarrow \theta(x) = 1 - v - s - D < 0$ and using that $s = D = 0$, $1 - v < 0$. This takes us to conclude that v, s and D are decreasing, so the dynamics points to the tetrahedron $\mathcal{T}$.
  - If we are inside the tetrahedron ($v < 1$), then $v + s + D < 1 \Rightarrow \theta(x) = 1 - v - s - D > 0$ and working like in the case that $v > 1$ we get that $1 - v > 0$. To determine the sign of $\dot{v}$ we have to distinguish between:
    - If $\alpha(1-\mu)(1-v) - \varepsilon < 0$,

$$\tilde{\theta}(x) = \theta(x)_{s=D=0} = (1-v) < \frac{\varepsilon}{\alpha(1-\mu)}.$$

      $\widetilde{\theta}(x)$ is greater than 1 if $\mu > \mu_*$ and smaller if $\mu < \mu_*$. Remember that $\mu = \mu_*$ is the bifurcation value that makes the origin to change its local stability and the existence or not of P. In this case v decreases and the system tends to $\frac{\varepsilon}{\alpha(1-\mu)}$. D is increasing here.
    - If $\alpha(1-\mu)(1-v) - \varepsilon > 0$, the results are similar to those in the previous case and we get

$$\tilde{\theta}(x) = \theta(x)_{s=D=0} = (1-v) > \frac{\varepsilon}{\alpha(1-\mu)}.$$

      Now $\dot{v} > 0$ and this means that the amount of viruses increases with time. D also increases.

– If $\theta(x) = 0$ and $s = D = 0$ we are in $(1, 0, 0)$. Imposing this in our system we obtain:

$$\dot{v} = -\varepsilon, \tag{25}$$
$$\dot{s} = 0, \tag{26}$$
$$\dot{D} = 0. \tag{27}$$

If we solve (25) we get

$$v(t) = -\varepsilon t + v(0),$$

where $v(0)$ is the initial quantity of virus. We have lineal extinction of the virus and it cease to have biological sense when v becomes negative.

Figure (33) sums up all of the ideas that we have just seen.

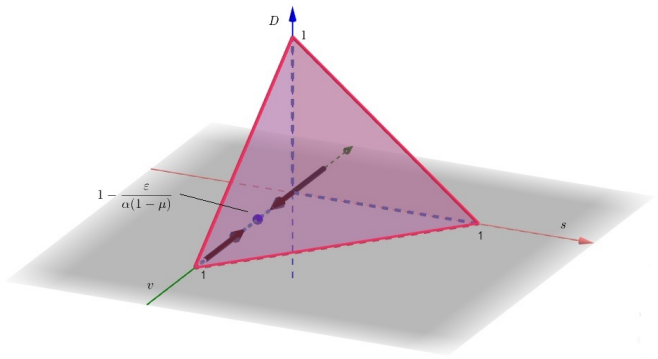

Figure 33: Dynamics on v-axis

- **Dynamics on s-axis.**
  Taking a point on the s-axis, that is $(0, s, 0)$ and replacing it in (1)-(3), we get to the following system:

$$\dot{v} = 0,$$
$$\dot{s} = -\varepsilon s,$$
$$\dot{D} = 0.$$

Solving the second equation, we conclude

$$s(t) = e^{-\varepsilon t} s(0),$$

with $s(0)$ the quantity of satellite at time 0. In this case s-axis is invariant for the dynamics and points to the origin due to the negativity of $\dot{s}$.

- **Dynamics on D-axis.**
  Taking an initial condition on the D-axis and working like in s-axis, we obtain that

$$D(t) = e^{-\varepsilon t} D(0),$$

  and, as in the previous case, this axis is invariant for the dynamics.

□

So far we have seen which is the dynamics of our system on the coordinate axes. Let study it in the different planes of $\mathcal{T}$.

Lemma 6.2 *On the coordinate planes, the vector field of our system points inwards the tetrahedron $\mathcal{T}$.*

Proof.

- **Dynamics on $\{v = 0\}$**
  If we replace $v = 0$ in the system we get

$$\begin{aligned} \dot{v} &= 0, & (28)\\ \dot{s} &= -\varepsilon s, & (29)\\ \dot{D} &= -\varepsilon D. & (30) \end{aligned}$$

  The first equation means that the plane $v = 0$ is invariant, so the dynamics does not change here. In biological terms, if we have not virus, it can not reproduce nor extinct. The satellite and the DIP decrease depending on the value of ε. Biologically, this decrease has sense because when there is no virus, the satellite and the DIP tend to extinct themselves. Although that, the decrease is not instantaneous because ε has a small value and s and D are the solutions of the ODE's (29) and (30):

$$\begin{aligned} s(t) &= e^{-\varepsilon t} s(0),\\ D(t) &= e^{-\varepsilon t} D(0), \end{aligned}$$

  where $s(0)$ and $D(0)$ mean the initial concentration of satellite and DIP.

- **Dynamics on $\{s = 0\}$**
  As we have seen in section 4.1, there is an equilibrium point in the invariant plane $s = 0$, $(v_0, 0, D_0)$. Now the system turns into

$$\begin{aligned} \dot{v} &= (\alpha(1-\mu)\,(1 - v - \eta_D D) - \varepsilon)v, & (31)\\ \dot{s} &= 0, & (32)\\ \dot{D} &= (\alpha\mu + \gamma D)\, v(1 - v - D) - \varepsilon D. & (33) \end{aligned}$$

As there is no satellite, we will study the dynamics in the plane (v, D). We are going to distinguish between the section above $v + \eta_D D = 1$ and the one which is below this line, as we can see in Figure (34), between $v + D = 1$, corresponding to $\theta(x) = 0$ with no satellite, and $v = 0$.

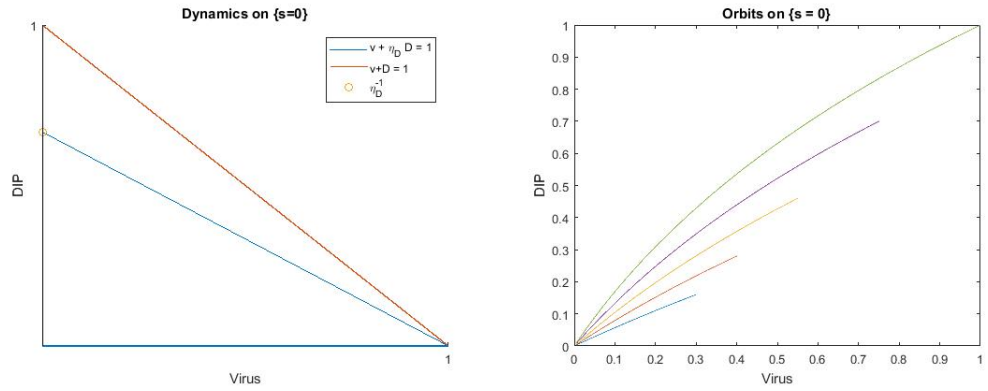

Figure 34: From left to right: studied sections on $\{s = 0\}$, and the orbits of the virus and the DIP for different initial conditions.

First of all we are going to study the lines $v + D = 1$ and $v + \eta_D D = 1$.

- If $v + D = 1 \Rightarrow 1 - v = D$ and (31)-(33) becomes

$$\begin{aligned} \dot{v} &= \alpha(1-\mu)\,(1-\eta_D)Dv - \varepsilon v, \\ \dot{s} &= 0, \\ \dot{D} &= -\varepsilon D, \end{aligned}$$

  which are all non positive, due to $\eta_D > 1$. These results take us to conclude that the virus and the DIP are decreasing.

- If $v + \eta_D D = 1 \Rightarrow 1 - v = \eta_D D$ and we get

$$\begin{aligned} \dot{v} &= -\varepsilon v, \\ \dot{s} &= 0, \\ \dot{D} &= (\alpha\mu + \gamma D)(\eta_D - 1)Dv - \varepsilon D. \end{aligned}$$

  1. If $D = 0$, since $s = 0$, we can reason like we have done studying the dynamics on v-axis in this same section.
  2. If $D \neq 0$, $\dot{D} = 0 \Leftrightarrow (\alpha\mu + \gamma D)v(\eta_D - 1) = \varepsilon$, and we have an exact value for D depending on ε:

$$D = D_\varepsilon = \frac{1}{\gamma}\left(\frac{\varepsilon}{v(\eta_D - 1)} - \alpha\mu\right),$$

Once we have studied the behaviour of our system on $v + D = 1$ and $v + \eta_D D = 1$ we want to study the region between these two lines. Let us recover the system:

$$\dot{v} = (\alpha(1-\mu)(1-v-\eta_D D) - \varepsilon)v, \tag{34}$$
$$\dot{s} = 0, \tag{35}$$
$$\dot{D} = (\alpha\mu + \gamma D)\, v(1-v-D) - \varepsilon D. \tag{36}$$

Firstly, as we want to know if in (34) $\dot{v}$ is positive or negative, we must differentiate two cases:

- $v + \eta_D D > 1$
  Due to the negativity of $\alpha(1-\mu)(1-v-\eta_D D)$, $\dot{v} < 0$, which means that v is decreasing.
- $v + \eta_D D < 1$
  Since $\alpha(1-\mu)(1-v-\eta_D D) > 0$, we will distinguish between $\alpha(1-\mu)(1-v-\eta_D D) > \varepsilon$ or $\alpha(1-\mu)(1-v-\eta_D D) < \varepsilon$ to determine the behaviour of $\dot{v}$.
  1. If $\alpha(1-\mu)(1-v-\eta_D D) < \varepsilon$ and we denote $\widetilde{\Omega}(x) = \Omega(x)_{s=0}$ we get that $\widetilde{\Omega}(x) < \frac{\varepsilon}{\alpha(1-\mu)}$. Besides,

  $$\frac{\varepsilon}{\alpha(1-\mu)} > 1 \Leftrightarrow \varepsilon > \alpha(1-\mu) \Leftrightarrow \mu > \mu_*$$
  $$\frac{\varepsilon}{\alpha(1-\mu)} < 1 \Leftrightarrow \varepsilon < \alpha(1-\mu) \Leftrightarrow \mu < \mu_*$$

  Notice that μ_* is the bifurcation value of μ that we have found in section 5 and that determines the nonlinear stability of the origin and the existence of P-points. In this case, the virus decreases.
  2. If $\alpha(1-\mu)(1-v-\eta_D D) > \varepsilon$ we obtain similar results working like in the previous case and we can conclude that v increases.

  Remark 6.3 *If $\alpha(1-\mu) = \varepsilon$ then $v+\eta_D D = 0$ and $\dot{v}$ is equal to 0, so v is constant. Biologically, it implies that the virus neither reproduces nor dies.*

Figure 34 shows the orbits on $s = 0$. To find these orbits we have integrated numerically system (31)-(33), using Runge-Kutta method of order 4 with different initial conditions, step 0.01 and parameters in Table 2.

- **Dynamics on {D = 0}**
  In this case the system becomes

$$\dot{v} = (\alpha(1-\mu)(1-v-\eta s) - \varepsilon)v, \tag{37}$$
$$\dot{s} = \beta s(1-v-s)v - \varepsilon s, \tag{38}$$
$$\dot{D} = 0. \tag{39}$$

Working like in the case that $s = 0$, as now there is no DIP, we study the dynamics in the plane (v, s). We differentiate between the section above $v + \eta s = 1$ and the one which is below this line, as we can see in Figure (35), between $v + s = 1$, corresponding to $\theta(x) = 0$ with no DIP, and $v = 0$.

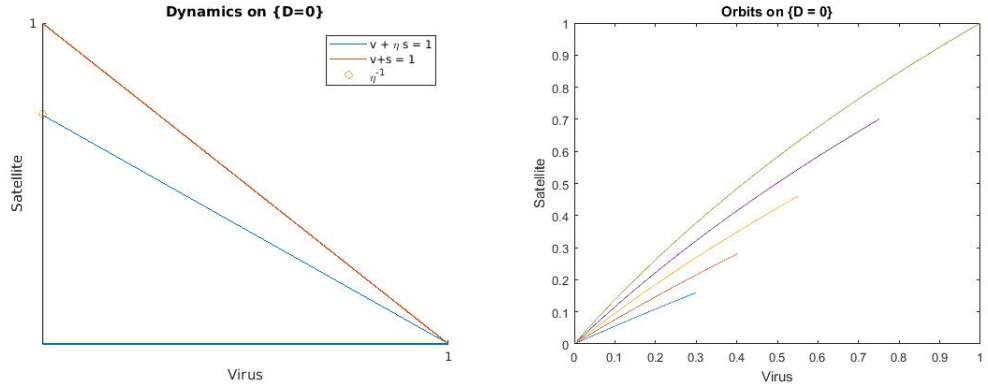

Figure 35: From left to right: studied sections on $\{D = 0\}$, and the orbits of the virus and the satellite for different initial conditions.

As we have done when $s = 0$, we study the behaviour of our system on $v + \eta s = 1$ and on $v + s = 1$.

- If $v + s = 1 \Rightarrow 1 - v = s$ and (37)-(39) becomes

$$\begin{aligned} \dot{v} &= \alpha(1-\mu)(1-\eta)sv - \varepsilon v, \\ \dot{s} &= -\varepsilon s, \\ \dot{D} &= 0, \end{aligned}$$

  which are all non positive, due to $\eta \geq 1$. These results take us to conclude that the virus and the satellite are decreasing.

- If $v + \eta s = 1 \Rightarrow 1 - v = \eta s$ and we get

$$\begin{aligned} \dot{v} &= -\varepsilon v, \\ \dot{s} &= \beta s(1-\eta)vs - \varepsilon s, \\ \dot{D} &= 0. \end{aligned}$$

  Again, due to $\eta \geq 1$, all the equations of the system are non positive.

Once we have studied $v + s = 1$ and $v + \eta s = 1$ we are going to distinguish two cases: the one when we are above $v + \eta s = 1$ and the one when we are under it. Recovering (37)-(39)

$$\dot{v} = (\alpha(1-\mu)(1-v-\eta s) - \varepsilon)v, \tag{40}$$

$$\dot{s} = \beta s(1-v-s)v - \varepsilon s, \tag{41}$$

$$\dot{D} = 0. \tag{42}$$

We want to study if in (40) $\dot{v}$ is positive or negative.

1. If $v+\eta s>1$, due to the negativity of $\alpha(1-\mu)(1-v-\eta s)$, $\dot{v}<0$ and v decreases.
2. If $v+\eta s<1$, since $\alpha(1-\mu)(1-v-\eta s)$ is positive, we distinguish between the next two cases:
   (a) If $\alpha(1-\mu)(1-v-\eta s)>\varepsilon$ and we denote $\widetilde{\Omega}(x)=\Omega(x)_{D=0}$, we get that $\widetilde{\Omega}(x)<\frac{\varepsilon}{\alpha(1-\mu)}$. Besides,

$$\frac{\varepsilon}{\alpha(1-\mu)}>1 \Leftrightarrow \varepsilon>\alpha(1-\mu) \Leftrightarrow \mu>\mu_*$$
$$\frac{\varepsilon}{\alpha(1-\mu)}<1 \Leftrightarrow \varepsilon<\alpha(1-\mu) \Leftrightarrow \mu<\mu_*$$

   In this case, v decreases.
   (b) If $\alpha(1-\mu)(1-v-\eta s)<\varepsilon$ we work as in the previous case and we get similar results. In this case the virus increases.

   Remark 6.4 *If $\alpha(1-\mu)=\varepsilon$ then $v+\eta s=0$ and $\dot{v}$ is equal to 0, so v is constant. Biologically, it means that the virus neither reproduces nor dies.*

Figure 35 shows the orbits on $\{D=0\}$. To find these orbits we have integrated numerically system (37)-(39), using Runge-Kutta method of order 4 with different initial conditions, step 0.01 and parameters in Table 2.

□

Up to here we have seen that the dynamics on the coordinate planes points to $\mathcal{T}$.

Lemma 6.5 *The dynamics on $\theta(x)=0$ points inwards the tetrahedron $\mathcal{T}$.*

- **Dynamics on $\{\theta(x)=0\}$**
  In this case, our system becomes

$$\dot{v} = (\alpha(1-\mu)(1-v-\eta s-\eta_D D)-\varepsilon)v, \tag{43}$$
$$\dot{s} = -\varepsilon s, \tag{44}$$
$$\dot{D} = -\varepsilon D. \tag{45}$$

  Equations (44) and (45) imply that the satellite and the DIP are decreasing in time depending on ε. Let study what happens with the virus.
  As $\theta(x)=0$ we have that $1-v-s-D=0$ and consequently $1-v=s+D$. Now (43) becomes

$$\dot{v}=\alpha(1-\mu)v\Omega(x)-\varepsilon v=\alpha v s D(1-\mu)(1-\eta)(1-\eta_D)-\varepsilon v\leq 0,$$

  due to $\eta_D>\eta\geq 1$ and $0<\mu\ll 1$. The equality is only reached at $(1,0,0)$ as a result of $\Omega(x)=0$ just at this point. We can conclude that the virus decrease.

□

This last fact let us affirm that all the dynamics of our system is inside the tetrahedron $\mathcal{T}$.

Let us recover the main system:

$$\dot{v} = \alpha(1-\mu)v\,\Omega(x) - \varepsilon v, \tag{46}$$

$$\dot{s} = \beta v s\,\theta(x) - \varepsilon s, \tag{47}$$

$$\dot{D} = (\alpha\mu v + \gamma v D)\,\theta(x) - \varepsilon D., \tag{48}$$

As we have seen in section 3, the plane $\{\Omega(x) = 0\}$ divides $\mathcal{T}$ in two regions:

(I) $\{\Omega(x) > 0\} \cap \{\theta(x) > 0\}$

(II) $\{\Omega(x) < 0\} \cap \{\theta(x) > 0\}$.

Theorem 6.6 *The dynamical system points to the origin in $\mathcal{T}$, provided that*

$$\Omega(x) < \frac{\varepsilon}{\alpha(1-\mu)}, \qquad v\theta(x) < \min(\frac{\varepsilon}{\beta}, \frac{\varepsilon D}{\alpha\mu + \gamma D}),$$

when we are in (I) and only imposing the right condition when we are in (II).

Proof.

(I) To determine the behaviour of the dynamical system we are going to distinguish if its equations are positive or negative.

(i) Equation (46) is negative provided that

$$\Omega(x) < \frac{\varepsilon}{\alpha(1-\mu)}, \tag{49}$$

As we have done in previous cases,

$$\Omega(x) > 1 \Leftrightarrow \mu > \mu_*$$

$$\Omega(x) < 1 \Leftrightarrow \mu < \mu_*$$

The virus decreases in (49).
On the other hand, (46) will be positive if $\Omega(x) > \frac{\varepsilon}{\alpha(1-\mu)}$ and we can reason similarly. In this case we conclude that the virus increases.

Remark 6.7 *If $\Omega(x) = \frac{\varepsilon}{\alpha(1-\mu)}$ there is no virus and we can work as in the plane $\{v = 0\}$.*

(ii) Equation (47) is negative provided that

$$v\theta(x) < \frac{\varepsilon}{\beta}, \tag{50}$$

and positive if $v\theta(x) > \frac{\varepsilon}{\beta}$. In the first case the amount of satellite decreases and in the second one it increases.

Remark 6.8 *If $v\theta(x) = \frac{\varepsilon}{\beta}$ we have no satellite and D is the solution of the ODE*

$$\dot{D} = D(\frac{\varepsilon\gamma}{\beta} - \varepsilon) + \frac{\alpha\mu\varepsilon}{\beta},$$

which is $D(t) = e^{(\frac{\varepsilon\gamma}{\beta}-\varepsilon)t}k + \frac{\alpha\mu}{\beta-\gamma}$, where k is a constant. D will be positive or negative depending on k and the relation between γ and β.

(iii) Equation (48) is negative provided that

$$v\theta(x) < \frac{\varepsilon D}{\alpha\mu + \gamma D}, \tag{51}$$

and it is positive when $v\theta(x) > \frac{\varepsilon D}{\alpha\mu+\gamma D}$. In the first case the concentration of DIP decreases and in the second one it increases.

Remark 6.9 *If $D = -\frac{\alpha\mu}{\gamma}$, the equation is always positive.*

Proof.
If $D = -\frac{\alpha\mu}{\gamma}$,

$$\dot{D} = (\alpha\mu v + \gamma v(-\frac{\alpha\mu}{\gamma}))\theta(x) + \frac{\varepsilon\alpha\mu}{\gamma} = \frac{\varepsilon\alpha\mu}{\gamma} > 0.$$

□

Remark 6.10 *If $v\theta(x) = \frac{\varepsilon D}{\alpha\mu+\gamma D}$, there is no DIP.*

(II) Working like in (I), the study with the satellite and the DIP is the same. The difference between the previous case and this is that the virus always decreases when $\Omega(x) < 0$. That means that the dynamical system will point to the origin provided that

$$v\theta(x) < \min(\frac{\varepsilon}{\beta}, \frac{\varepsilon D}{\alpha\mu + \gamma D}),$$

and no matter which is the value of $\Omega(x)$ whenever it is negative.

□

Lemma 6.11 *The dynamics on* $\{\Omega(x) = 0\}$ *points to the origin provided that*

$$v\theta(x) < \min(\frac{\varepsilon}{\beta}, \frac{\varepsilon D}{\alpha\mu + \gamma D}).$$

Proof.

- **Dynamics on $\Omega(x) = 0$**
  The system becomes

$$\dot{v} = -\varepsilon v, \tag{52}$$
$$\dot{s} = \beta v s\theta(x) - \varepsilon s, \tag{53}$$
$$\dot{D} = (\alpha\mu + \gamma D)v\theta(x) - \varepsilon D. \tag{54}$$

  As v is the solution of (52) and it is

$$v(t) = e^{-\varepsilon t}v(0),$$

  with v(0) the initial quantity of virus it is clear that v decreases in time.

  Moreover, as when $\Omega(x) = 0$ it is also true that $\theta(x) > 0$, we can recover Theorem 6.6 and conclude that the dynamics on this plane points to the origin when $v\theta(x) < \min(\frac{\varepsilon}{\beta}, \frac{\varepsilon D}{\alpha\mu+\gamma D})$.

□

7 Conclusions

The main objective of this research is to develop a model based on ordinary differential equations to investigate the dynamics of the Hepatitis B virus, which carries RNA satellites, and the DIPS generated by it. The virus, the satellite and the DIPs, denoted by v, s and D, respectively, have only biological meaning if they are non negative. Furthermore, we have seen that tetrahedron $\mathcal{T}$, determined by the coordinate planes and $\{\theta(x) = 0\} \equiv \{v + s + D = 1\}$, contains long-time dynamics and it is positively invariant under the flow of our system.
An important part of this work has been to determine the equilibrium points and to study their stability. We have found three types of equilibrium points:

- the origin $O = (0, 0, 0)$, which means all-virus extinction. This type of equilibrium involves, if stable, the extinction of the three virus types,

- virus satellite equilibrium $P = (v_0, 0, D_0)$, provided that

$$\mu < \mu_* = 1 - \frac{\varepsilon}{\alpha},$$

  which involves, whenever stable, the coexistence of the standard virus with its DIPs and the extinction of the virus satellite.

- all-virus coexistence $Q = (v_1, s_1, D_1)$, with necessary conditions to exist

$$\beta > \gamma, \qquad \eta_D \frac{\alpha\mu}{\beta - \gamma} + \frac{\varepsilon}{\alpha(1 - \mu)} < 1,$$

  and the existence of $v_1 = A - \eta s_1$, with s_1 any root of a determined polynomial of degree 2. Condition in the left means satellite replicate rate must be greater than DIPS one, and condition in the right takes us to conclude that Q exists when $\mu < \mu_*$, the condition of P-points to exist. From here we conclude that Q-points, if they exist, coexist with P-points. Biologically, all-virus coexistence is the worst equilibrium case since the harmful medical consequences.

As our system is not linear, Hartman-Grombann's theorem has been useful to determine its stability, due to it states a relation between a non-linear system and its linearized one. After studying the stability of our system we can conclude that:

- When $\mu \in (0, \mu_*)$ the origin is an unstable node and P-points exist. From μ_*, P-points disappear (if they exist) and the origin becomes asymptotically stable.

- If $\mu = \mu_*$, P-points collide and become the origin.

- If $v(1 - v - D) > \frac{\varepsilon}{\beta}$, P is unstable. Numerically we have found some bifurcation values that make P-points to change their stability.

- One of the necessary conditions to the existence of Q-points is $\mu < \min(\mu_*, \frac{\beta-\gamma}{\alpha\eta_D})$. Numerically, as in P-points, we have found bifurcation values where the stability of Q changes. We have found that the bifurcation values of Q, in most cases, have an important role in the stability of P.

Studying the dynamics onto the border of $\mathcal{T}$ we have seen that it points inwards the tetrahedron despite inside it, on v-axis, where the dynamics points to $\frac{\varepsilon}{\alpha(1-\mu)}$. Moreover, s and D axes are invariant. Finally, we can conclude the hepatitis B system tends to the origin in $\mathcal{T}$ (biologically, to the extinction) provided that

$$\Omega(x) < \frac{\varepsilon}{\alpha(1-\mu)}, \qquad v\theta(x) < \min\left(\frac{\varepsilon}{\beta}, \frac{\varepsilon D}{\alpha\mu + \gamma D}\right),$$

if we are in $\{\Omega(x) > 0\} \cap \{\theta(x) > 0\}$ and only imposing the second one in $\{\Omega(x) < 0\} \cap \{\theta(x) > 0\}$ or in the plane $\Omega(x) = 0$.

As far as we know, this project is the first attempt to describe the dynamics of virus-satellite-DIP system. It is based on a real dynamical system of the competence between these three types of viruses. Although that, it is just a first step in the study since in real life the system becomes harder, but it could be useful to understand the main dynamics of the system.

Personally, the most beautiful part of this work has been to see a real biological application of the theoretical mathematics that I have studied during the degree, as from subjects like Ordinary Differential Equations or Numerical Methods for ODEs. In addition, I have not studied Dynamical Systems and it has been an interesting challenge for me to learn the basics of this subject.

References

[1] Chung-Chi, H., Yau-Hieu, H., Na-Sheng, L. *Satellite RNAs and Satellite viruses of plants. Viruses 1(3):* 1325-1350 (2009)

[2] Hepatitis D virus: http://web.stanford.edu/group/virus/delta/2005/

[3] Von Magnus, P.: *Incomplete forms of influenza virus.* Adv. Virus. Res. 2, 5979 (1954)

[4] Huang, A.S.: *Defective interfering viruses.* Annu. Rev. Microbiol. 27, 101117 (1973)

[5] Kool, M., Voncken, J.W., Vanlier, F.L.J., Tramper, J., Vlak, J.M.: *Detection and analysis of Autographa californica nuclear polyhedrosis-virus mutants with defective interfering properties.* Virology 183, 739-746 (1991)

[6] Wickham, T.J., Davis, T., Granados, R.R., Hammer, D.A., Shuler, M.L., Wood, H.A.: *Baculovirus defective interfering particles are responsible for variations in recombinant protein-production as a function of multiplicity of infection.* Biotechnol. Lett. 13, 483488 (1991)

[7] Pijlman, G.P., van den Born, E., Martens, D.E., Vlak, J.M.: *Autographa californica baculoviruses with large genomic deletions are rapidly generated in infected insect cells.* Virology 283, 132138 (2001)

[8] Giri, L., Feiss, M.G., Bonning, B.C., Murhammer, D.W.: *Production of baculovirus defective interfering particles during serial passage is delayed by removing transposon target sites in fp25k.* J. Gen. Virol. 93, 389399 (2012)

[9] King, L.A., Possee, R.D.: *The Baculovirus Expression System.* University Press, Cambridge (1992)

[10] Lee, H.Y., Krell, P.J.: *Reiterated DNA fragments in defective genomes of Autographa californica nuclear polyhedrosis virus are competent for AcMNPV-dependent DNA replication.* Virology 202, 418429 (1994)

[11] Pijlman, G.P., Dortmans, J., Vermeesch, A.M.G., Yang, K., Martens, D.E., Goldbach, R.W., Vlak, J.M.: *Pivotal role of the non-hr origin of DNA replication in the genesis of defective interfering baculoviruses.* J. Virol. 76, 56055611 (2002)

[12] Pijlman, G.P., van Schijndel, J.E., Vlak, J.M.: *Spontaneous excision of BAC vector sequences from bacmid-derived baculovirus expression vectors upon passage in insect cells.* J. Gen. Virol. 84, 26692678 (2003)

[13] Palma, E.L., Huang, A.: *Cyclic production of vesicular stomatitis virus cause by defective interfering particles.* J. Infect. Dis. 129, 402410 (1974).

[14] Stauffer Thompson, K.A., Yin, J.: *Population dynamics of an RNA virus and its defective interfering particles in passage cultures.* Virol. J. 7, 257266 (2010)

[15] Terr, S., Petit, M-A., Brchot, C. *Defective Hepatitis B Virus particles are generated by packaging and reverse transcription of spliced viral RNAs in vivo.* J. Virol. 65(10), 5539-5543 (1991)

[16] Rosmorduc, O., Petit, M-A., Pol, S., Capel, F., Bortolotti, F., Berthelot, P., Brechot, C., Kremsdorf, D. *In vivo and in vitro expression of defective hepatitis B virus particles generated by spliced hepatitis B virus RNA.* Hepatology 22(1), 10-19 (1995)

[17] Szathmry, E.: *Cooperation and defection playing the field in virus dynamics.* J. Theor. Biol. 165, 341356 (1993)

[18] Zwart, M.P., Piljman, G.P., Sardanys, J., Duarte, J., Janurio, C., Elena, S.F. *Complex dynamics of defective interfering baculoviruses during serial passage in insect cells.* J Biol Phys 39:327342 (2013) DOI 10.1007/s10867-013-9317-9

[19] Bangham, C.R.M., Kirkwood, T.B.L.: *Defective interfering particles effects in modulating virus growth and persistence.* Virology 179, 821826 (1990)

[20] Kirkwood, T.B.L., Bangham, C.R.M.: *Cycles, chaos, and evolution in virus cultures a model of defective interfering particles.* Proc. Natl. Acad. Sci. USA 91, 86858689 (1994)

[21] Ramirez, R.: https://mat-web.upc.edu/people/rafael.ramirez/edos/sl.pdf

[22] Transcritical bifurcation: https://en.wikipedia.org/wiki/Transcritical_bifurcation